2018-01-01

Magnetotelluric Analysis Of Central Kenya Kenyan Rift Volcanoes For Geothermal Development

Anna Wairimu Mwangi
University of Texas at El Paso, anna.mwangi@gmail.com

MAGNETOTELLURIC ANALYSIS OF CENTRAL KENYA KENYAN RIFT VOLCANOES FOR GEOTHERMAL DEVELOPMENT

ANNA WAIRIMU MWANGI

Doctoral Program in Geological Sciences

APPROVED:

Laura Serpa, Ph.D., Chair

Kevin Mickus, Ph.D.

Aaron Velasco, Ph.D.

Hector Gonzalez, Ph.D.

Stanley Mubako, Ph.D.

Charles Ambler, Ph.D.
Dean of the Graduate School

Dedication

To my father John Mwangi Nduati who at a young age taught me about concepts, my mom Mary Wambui Mwangi who taught me to read and write, my husband Atanasio Njue for the rock solid steady support and to my son Ngivavey Njue who defied all odds into existence; curious as a cat and teaching me to do it all.

MAGNETOTELLURIC ANALYSIS OF CENTRAL KENYA RIFT VOLCANOES FOR GEOTHERMAL DEVELOPMENT

by

ANNA WAIRIMU MWANGI, MS, BS.

DISSERTATION

Presented to the Faculty of the Graduate School of

The University of Texas at El Paso

in Partial Fulfillment

of the Requirements

for the Degree of

DOCTOR OF PHILOSOPHY

Department of Geological Sciences

THE UNIVERSITY OF TEXAS AT EL PASO

December 2018

Acknowledgements

I credit the success of this study to many people who have played various roles and I may not fit all in this page. My sincere gratitude to my advisor Dr. Serpa, who met me in Kenya who not only inspired me but she also gave me this wonderful opportunity to study geophysics at UTEP. She has been a great mentor; teacher, friend and I appreciate the many wonderful conversations that have opened my mind and broadened my perspective. My gratitude goes to Dr. Kevin Mickus has been very instrumental in data processing, analysis, fieldwork survey designs and the many fruitful discussions that have helped shape the study. Thanks are due to Dr. Aaron Velasco, Dr. Hector Gonzalez, Dr. Stanley Mubako and Dr. Terry Pavlis for the reviews and ideas to improve the work. My appreciation to Dr. Elizabeth Anthony for providing me useful references and with Dr. Peter Omenda, Dr. Nicholas Mariita, Dr. Ben Bruner and Joel Muhanga provided insightful forum discussions about the Kenya rift volcanoes. Thanks are due to Dr. Diane Doser for the great support and to my dear friend Anna Shaughnessy who has been a great mentor, cheering me on every step of the way. I appreciate Carlos Montana for the awesome tech support to help me accomplish this study and Galen Kaip for the best short courses in geophysical instrumentation. I thank Kenya Electricity Generating Company for providing datasets and travel support and the Geological Sciences department UTEP for Teaching assistantship as well as field support.

David and Sandra Rascon and their family (Alex, Lisa, Aiden, Maura, the Morales) have become my family in El Paso and I thank you for the friendship and love. To Godparents Geraldo and Sarah thank you for the love and many memories we made in Kenya and now in El Paso, your children are such a delight. Kathy and Ronald Stone I am touched by your kindness and love. Dr. Annette Veilleux, Chanel Perez, Claire Bailey, Sandy Hardy, Ashley Nauer, Sarah Olivas, Valeria, Amber, Syprose and all my friends and colleagues at the department; thank you for the laughs, team work and just being yourself.

I appreciate my husband Atanasio Njue and my son Ngivavey Njue for the love, patience, sacrifice and unwavering support. I am indebted to my parents John Mwangi and Mary Wambui, my first teachers, Jere Kamau who is amazing and everyone walked with me in this journey. Even though my father got ill during the course of my doctoral studies, I know a sure that he is especially pleased with my accomplishment.

This dissertation was submitted to the supervising committee on 12th November 2018.

Abstract

High temperature geothermal resources are vast along rift margins because of emplacement of magma in shallow crust. This is the case along the Kenyan Rift valley also known as the Gregory Rift. It is the Eastern arm of the East African rift and a chain of volcanoes along the rift graben characterizes it. We use (MT) magnetotelluric method to image beneath the peralkaline province of the Kenya Rift i.e. Olkaria, Eburru, Badlands, and Longonot volcanoes. The resistivity structure shows active geothermal activity happening at the upper 3km from the subsurface as evidenced by low resistivity cap rock comprised of low resistivity minerals. The cap is significantly thick on the Longonot volcano than any of the other case study areas depicting a shallow magma heat source closer to the surface compared to the rest of the volcanoes. We observe significantly large high resistivity blocks, which are faulted and intruded by magma. The depth to the large magma reservoir is about 8-10km below surface and it upwells to a shallow depth of 5-6 km, however, it much shallower at Mt Longonot occurring at about 3km below surface. A deep connection of magma intrusions in Olkaria Domes and Longonot strato volcano is observed. Eburru and Badlands have two major heat sources, the large one is associated with Eburru crater and the other is located northwest side of Badlands. The geothermal reservoirs observed in the peralkaline province are high temperature systems because they are supported by shallow magma intrusions. Major faults structures present in these fields play a significant role in fluid movement controlling hot up flows and circulation within the reservoirs.

Table of Contents

Acknowledgements..... v

Abstract..... vii

Table of Contents..... viii

List of Figures..... x

Chapter 1: Exploring Eburru- Badlands Volcanic Region For Geothermal Potential using Magnetotellurics 1

Abstract 1

1.1 Introduction 1

1.2 Electromagnetic 6

methods 1.3 Results 11

1.4 Discussions 13

1.5 Conclusion 15

1.6 Acknowledgments 17

1.7 References 18

Chapter 2: Characterization of the geothermal system of the Mt. Longonot Volcano and Olkaria Domes volcanic field, Kenyan Rift System 20

Abstract 20

2.1 Introduction 20

2.2 Magnetotelluric (MT) method 23

2.3 Results 27

2.4 Discussion of Results 33

2.5 Conclusions 33

2.6 Acknowledgements 34

2.7 References 35

Chapter 3: Dimensionality Analysis Of The Olkaria Geothermal Field, East Africa Rift.....37

Abstract 37

3.1 Introduction 38

3.2 Electromagnetic Methods 40

3.3 Results 42

3.3 Discussions and conclusions 45

3.4 Recommendations 48

3.5 References 49

Vita 51

List of Figures

Figure 1.1: Location map of Eburru and Badlands volcanic fields. (DEM sourced from www.opentopography.org and world map sourced from Googlemaps) 3
Figure 1.2: Geological map and structural map of the Eburru and Badlands fields. (DEM sourced from www.opentopography.org) 4
Figure 1.3: A geological model proposed for the rift volcanoes from integrated seismic, gravity and drill core information (Adapted from Simiyu, (2000), highlighted is Eburru and Badlands volcanic region). 5
Figure 1.4: Eburru geothermal field and Badlands area. 9
Figure 1.5: Resistivity depth slice at -2000m elevation derived from 1D inversion of MT data. The resistivity distribution with depth shows low resistivity anomalies in a northwest southeast orientation. 2D inversion was performed along the selected profiles. Little black triangles indicate location of MT sounding. 10
Figure 1.6: East-west 2D resistivity profile along Eburru crater crossing well 1. 11
Figure 1.7: East-west 2-D profile along Badlands area, north of Eburru massif. 12
Figure 1.8: 2-D resistivity profile NW-SE starting at Badlands (NW) and Eburru (SE). A low resistivity structure is observed in the Badlands area. 13
Figure 1.9: Geophysical signature and temperature regime in a geothermal set up (Adapted from (Pellerin et al., 1996; Cumming, 2009). The conductive clays occur close at the top of the reservoir. 14
Figure 1.10: A modified geological model incorporating magnetotelluric data seismic, gravity and drill core information (Modified from Simiyu, (2000). Eburru and Badlands volcanic region is highlighted in the red box. This model shows crustal thinning by magma, which has been shown to be 8-12km below surface. 17
Figure 2.1: Location map of the Mt Longonot and Olkaria Domes within Kenya Rift valley. (DEM sourced from www.opentopography.org) 21
Figure 2.1b: Geological map of Mt Longonot and part of Olkaria Domes. The major faults observed are a fracture zone referred to as the Tecto volcanic axis. 24
Figure 2.2: Dimensionality of Mt. Longonot and Olkaria Domes volcanoes. 26
Figure 2.3: 1D resistivity slice at -2000m elevation showing low resistivity anomalies at the eastern flank of Longonot and to the west of Longonot outer caldera. Line profiles (A-G) were selected and 2D inversion performed; black triangles are the MT data locations. 27
Figure 2.4: Profile A-A'- 2D inversion resistivity profile northwest area south of Olkaria Domes to northeast side of Longonot. 28
Figure 2.5: Profile B-B', Olkaria Domes (west) - Longonot (east) 2D inversion resistivity profile. 29
Figure 2.6: Profile C-C', Olkaria Domes (west) - Longonot (east) 2D inversion resistivity profile. 30
Figure 2.7: Profile D-D'- 2D inversion resistivity profile southwest, area south of Olkaria Domes to northeast side of Longonot. 31
Figure 2.8: 2D inversion showing 3 parallel profiles from south to north 2.8a) profile E-E' 2.8b) profile F-F' and 2.8c) profile G-G' 32
Figure 3.1: Location of the a) East Africa Rift system (Min and Hou, 2018) and b) central Kenya rift volcanoes including the Olkaria volcanic system (Omenda, 1998). 39
Figure 3.2: Dimensionality of Olkaria geothermal field, the points are MT sounding locations; various symbols show dimensionality type. The coordinate values: - latitude (x axis) and longitude (y axis) in degrees. 42
Figure 3.3: Resistivity slice at sea level approximately 2km depth from the surface. NW-D and S-NE profiles are the locations of two MT inverse models. The triangles are the location of MT stations. Dashed lines are faults. (UTM (km) and latitude – longitude (degrees) coordinates) ... 43
Figure 3.4: 2D inverse model along profile S-NE (Figure 3). The deeper high resistivity values are interpreted as high heat values above the magma chamber. The shallow magma intrusion is

mapped at 6-7 km deep, the blue arrow shows peak of a doming resistivity core with doming elevation at the surface..... 44
Figure 3.5: 2D inverse model along profile NW-D (Figure 3). The deeper low resistivity values are interpreted to be heat values above the magma chamber with an absence of the high resistivity core on the NW sector. The magma intrusion is mapped at 6-7 km deep. 45
Figure 3.6: Generalized resistivity and temperature response over hydrothermally altered basaltic crust in Iceland (Flovenz et al., 1985)..... 46

Chapter 1: Exploring Eburru- Badlands Volcanic Region For Geothermal Potential using Magnetotellurics

Abstract

In high temperature geothermal fields, the location of the heat source is the most critical information needed to determine how to utilize the heat for power generation. In Eburru, Kenya, we apply electromagnetic methods to map the reservoir and the location of the heat source(s) to site wells for optimum electricity generation. Magnetotelluric (MT) methods indicate the Eburru massif has more than 1 intrusion and the largest is located on the west side of the main Eburru inferred crater. The results suggest that geothermal well 1, a wellhead power plant producing 2.5 Mwe, is tapping a geothermal reservoir located above a high temperature dyke along a boundary fault structure. At depth, a very large magma source ~ 8 to 12 km is observed and it is postulated to be the originating from the East side of the volcano i.e. toward the axis of the rift. That deep source appears to provide magma to several shallow dykes in the region, along linear structures i.e. faults but magma transport may be blocked near the center of the massif by a large plug of cooled high resistivity material.

1.1 Introduction

The Eburru geothermal field is located on a massif volcano in the central section of the Kenya rift in a volcanic province north of Olkaria (Figure 1.1). Eburru became of interest for power production because it has spectacular geothermal manifestations including altered red grounds comprised mostly of conductive red and brown clays as well as sulfur-laced fumaroles with the characteristic smell of hydrogen sulfide indicating shallow heat source. Fumaroles occur in a linear profile around the field suggesting dyke intrusions along faults, and hot springs and steaming grounds are also a common occurrence. Further the surface measurement indicated a anomalous high heat gradient. Geothermal grass (*Fimbristylis exilis*), a plant observed to grow only in geothermal fields (Wetang'ula, 2012) is very common in Eburru field.

Six exploration wells were drilled on Eburru between 1989-1991 based on studies by the Kenya Electricity Generating Company. A wellhead power plant currently produces 2.5 MWe of energy from one of the exploration wells (Well 1) and this suggests there is more potential to scale up geothermal development in the region. Reservoir well completion tests of the other 5 exploration wells showed high temperature fluids were present throughout the region but they also showed signs of mixing of meteoric cold with geothermal hot water below a depth of 2 km. The heat source and pathways for fluid flow were not identified in this initial study and development did not continue after the initial well was exploited.

Despite the evidence for cool meteoric water circulating and recharging the system at depth, the area has a severe water crisis because there is no portable surface water available for drinking. Thus, communities living in the area use rudimentary condensers to collect droplets of water condensed from steam for drinking and domestic use. Geothermal development can help the Eburru community by in many ways such as producing electricity to be used locally which will scale up existing economic activities e.g. growing of pyrethrum (main ingredient in pesticide production), where locals have applied direct use of geothermal heat to dry the flowers, also it can transform the area to be a tourist destination. Mapping for geothermal resources will provide solutions to the potable water crises facing the community by delineating sources of meteoric water.

In order to expand geothermal production in the Eburru field, electromagnetic data, (MT and TEM (transient electromagnetic)) were collected in 2016 and used with other existing older data sets (Mwangi, 2013; Omiti, 2013) to identify possible heat source(s), define the reservoir system and the role of the prominent faults observed in the field. The data shows shallow and deep magma sources emplaced on the east of the Eburru crater and to the west of the Badlands area.

1.1.1 Background

Eburru volcano is part of the series of volcanoes that formed in the Quaternary period due to extension in the East African rift system. East Africa began rifting in the early Miocene but the Kenyan section did not begin to rift until the Oligocene (Baker et al., 1972). Volcanism along the rift is due to a thinning lithosphere, (Simiyu, 2000; Simiyu and Keller, 2001a) where magma is emplaced in a metamorphic basement (Baker and Wohlenberg, 1971; Simiyu and Keller, 2001a) under the volcanoes.

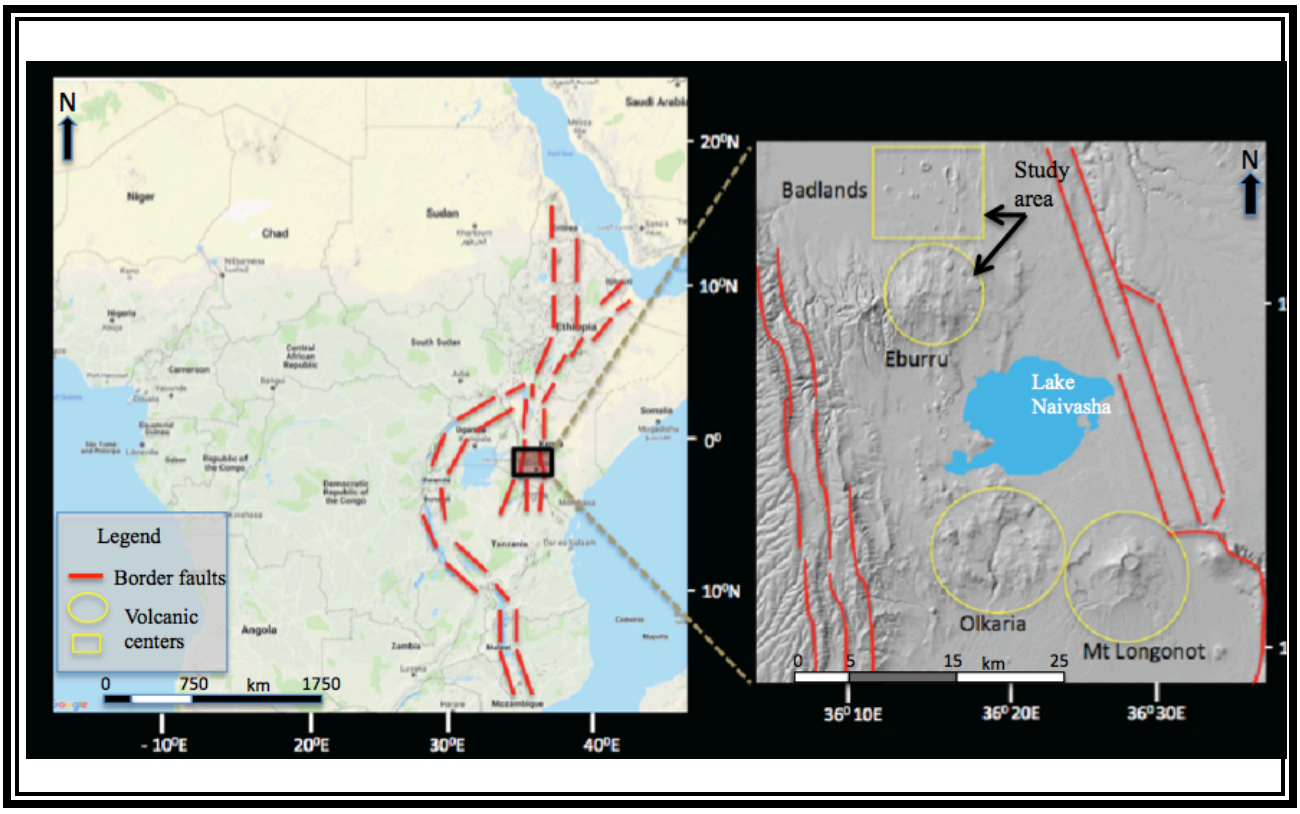

Figure 1.1: Location map of Eburru and Badlands volcanic fields. (DEM sourced from www.opentopography.org and world map sourced from Googlemaps)

The average elevation of the Eburru massif is 2811m. The massif forms the northern boundary of the Lake Naivasha watershed (Clarke 1990), a catchment area postulated to contribute to recharging the Eburru geothermal system (Arusei, 1991). Badlands area, located

north of Eburru volcano, includes numerous small craters occurring along prominent north-south oriented faults and fissure lava flows of older and newer basalts. To the south is Ndabibi plains, characterized by cinder cones covered with pyroclasts comprised mostly of pumice and ash. The main rocks around Eburru are trachytes, pantellerites and pyroclasts. The eruption sequences in Eburru indicates an evolved magma comprised of trachyte and latest eruption is comprised of pantellitic rhyolites (Clarke et al., 1990; Lagat, 2003). The significance of this volcano is that the characteristic magma is well hydrated and peralkaline (iron and potassium oxides concentration more than aluminum oxides as well as higher concentration of halogens) making the magma melt light and easy to flow (Scaillet, 2001; Gioncada and Landi, 2010).

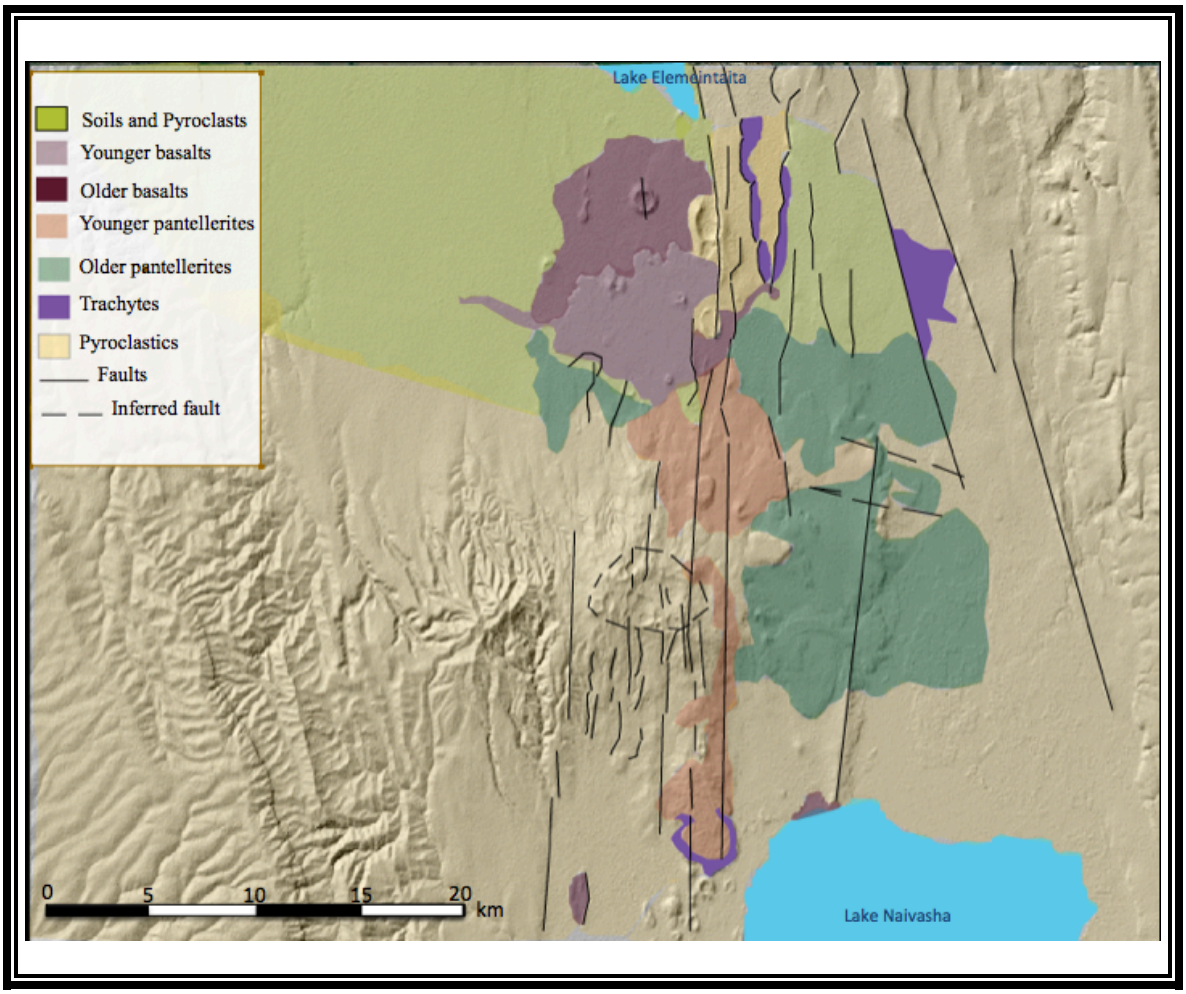

Figure 1.2: Geological map and structural map of the Eburru and Badlands fields. (DEM sourced from www.opentopography.org)

1.1.2 Previous Geophysical Studies

Geophysical studies around Eburru and Badlands area have focused on as part of a large study of the East African rift system. Local gravity studies by Simiyu, (1990) showed structurally controlled high density bodies and regional gravity studies showed anomalous high density anomaly between Lake Elemeintaita and Mt Suswa (Maguire et al., 1994; Simiyu and Keller, 2001b) and this was attributed to dyke swamps mostly around Eburru field. Regional seismic experiment such as KRISP a seismic line from Lake Baringo to Magadi was not adequate enough to explain the phenomena. A geologic model was proposed to explain the features under the volcanoes. The anomalous bodies are the intrusions that are emplaced in the reworked Precambrian basement causing the thinning of the lithosphere Simiyu, (2000).

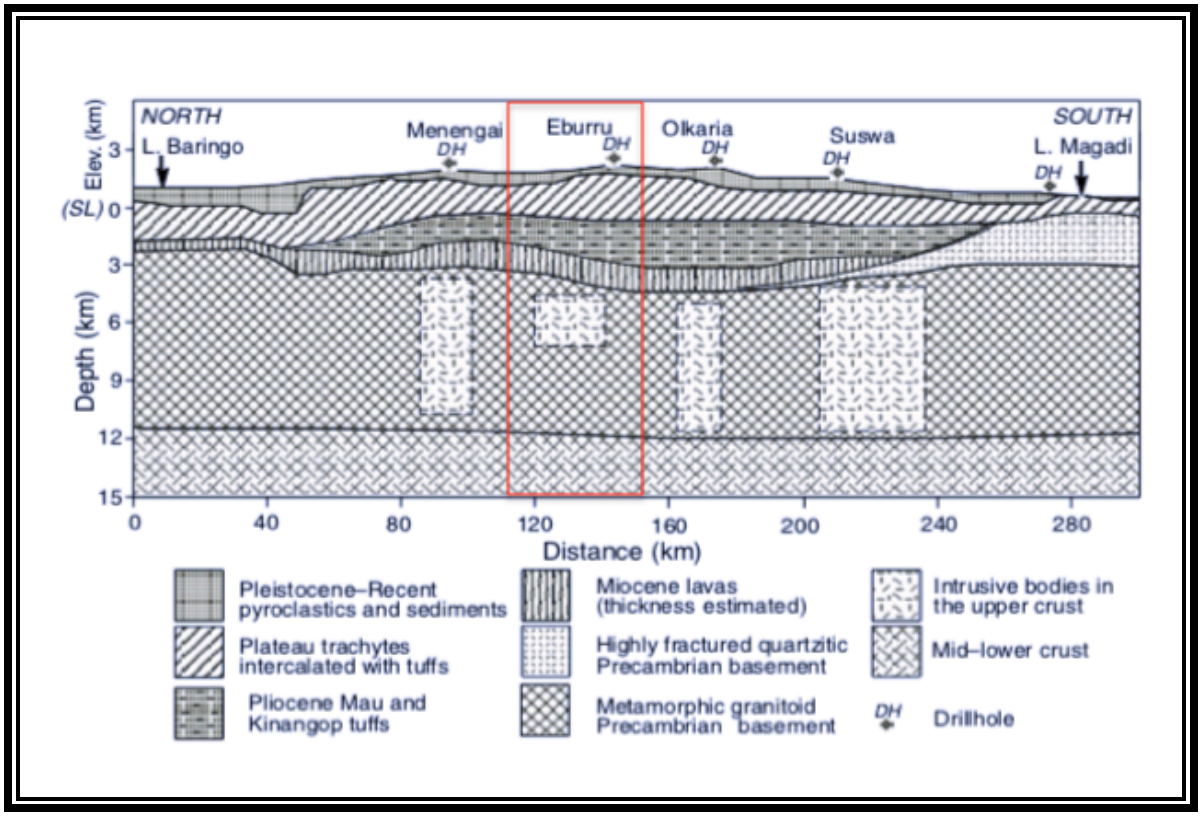

Figure 1.3: A geological model proposed for the rift volcanoes from integrated seismic, gravity and drill core information (Adapted from Simiyu, (2000), highlighted is Eburru and Badlands volcanic region).

Applications of other geophysical methods like electromagnetics are very useful to resolve or improve resolution where other methods may not be sufficient. Magnetotelluric studies done around Eburru crater showed a high temperature system from 1-D inversion results of the MT data. The are around well 1 indicated high temperature signature that is fault controlled (Mwangi, 2013; Omiti, 2013). Application of MT can assist to image the crustal anomalous crustal conditions around the peralkaline province.

1.2 Electromagnetic methods

To map the subsurface for deep-seated intrusions and structural controls on the geothermal system we applied electromagnetic methods because they are ideal for probing deep into the subsurface and high resolution imaging of features of major interest to this study. Magnetotelluric (MT) and central loop transient electromagnetic method (TEM) were used in the Eburru geothermal field and Badlands area with data coverage of approximately 150km^2.

1.2.1 MT method

The MT method relies on natural electromagnetic signals that originate from solar winds and distant lightning. The farther away the source is the longer the wavelength of the signals will be. When the waves reach the surface of the earth they dissipate into the ground vertically where the depth of wavelength attenuation is dependent on the electrical properties of the surface. Long period waves will attenuate at greater depths than short period waves as determined by the skin depth equation (Berdichevsky and Dmitriev, 2008).

$\delta = 500 \sqrt{T\rho}$ where δ = Skin depth (km), ρ = Resistivity (Ohm-m), T = Period (s).

The MT data were collected using 2 pairs of electrodes placed 60 m apart on the ground in an east-west and north-south direction. This was done to measure the electric field (E) and an orthogonal magnetic sensor was used to measure the corresponding magnetic field (H). A problem with the MT method is that inhomogeneity at shallow depths distorts the electric field hence affecting the impedance tensor and the result is a static shift in the resistivity curves (Árnason, 2018).

1.2.2 TEM method

The TEM method (central loop) involves laying out a square loop (200m by 200m) of wire with a receiver sensor placed in the middle of the loop. A current is passed along the loop and sporadically shut off. The decaying magnetic field associated with the induced current, generates eddy currents in the ground and the receiver sensor records the voltage to determine the electrical properties of the ground (Stephen et al., 2003). Since TEM method involves injecting current into the ground and measuring a decaying magnetic wave to calculate the apparent resistivity curves it avoids direct measurements through electrodes on the ground where inhomogeneity introduce static shift as is the case in MT hence the static shift. The maximum depth of penetration is determined by how deep the current disseminates into the ground and hence probes shallow depths.

$\delta = \sqrt{(2T/\mu\sigma)} \approx 1.26 \times \sqrt{(\rho T)}$

where δ = Skin depth (m), ρ = Resistivity (Ohm-m), $T = 10^{-6}$seconds

1.2.3 Data collection and Processing

These data are acquired as a time series recorded for an average of 22 hours at each site using Phoenix Geophysics MTU-5A™ MT instruments. To minimize on the noise a remote reference was chosen to simultaneous collect data and match acquisition with all the data sets. The data is then processed with the remote station and the results are objective apparent resistivity values. The remote station is chosen to be sufficiently far away to make sure the noise in the magnetic field is uncorrelated. This enables improvement of signal to noise (Gamble et al., 1979). The time series data recorded were transformed into the frequency domain and processed further to obtain apparent resistivity information at frequency ranges of 0.1-0.001 Hz using software from the Phoenix Geophysics™ suite. The data were then represented as apparent resistivity curves against period and as each data point was represented as cross powers to allow removal of outliers. The results were converted to electronic data interchange (EDI) format for further analysis and modeling. The overall data quality is excellent and static shift correction was performed on transverse electric (TE) and transverse magnetic (TM) curves before

modeling. A 1-D layered model of the invariant of TE and TM were used as a starting model for Occam inversion and the root means square error averaged at less than 1.0% (between the layered calculated model and the Occam model).

1.2.4 Dimensionality

Dimensionality is the change in alignment of a conductor and is caused by hydrothermal activities, micro fracturing or secondary mineralization. To determine the dimensionality of Eburru we used Waldim code (Martí et al., 2009, 2010) to resolve the directionality of the electrical signals caused by local structures and the McNeice and Jones, (2001) code to determine the regional strike. Dimensionality and directionality (strike) for the Eburru and adjacent Badlands area is represented in 4 period bands (Figure 1.4), where wavelength is measured in seconds, short periods correspond to conditions at shallow depth and longer periods represent greater depths.

The local strike is mainly east northeast for the 0.1-1 s period band but as the period increases the trend shifts to north-south and east-west orientations. It appears that the strike is mostly influenced by regional structures such as the prominent north-south trending faults at Badlands that intersect east west minor faults hence forming crosshatch network of structures (Arusei, 1991).

The dimensionality of the data periods 0.1-1 s is mainly 1-D around the Badlands area however near the Eburru main crater the data shows a 3-D trend. At period bands 1-10 s the result is ambiguous, either 3-D/2-D or 3-D/1-D. At longer period bands 10 - >100 sec the data is predominantly 3-D (Figure 1.4).

Resistivity slice was made at -2000m elevation to give a preliminary view of resistivity variation with depth. Figure 1.5 shows the low resistivity anomalies in Badlands and around Eburru crater.

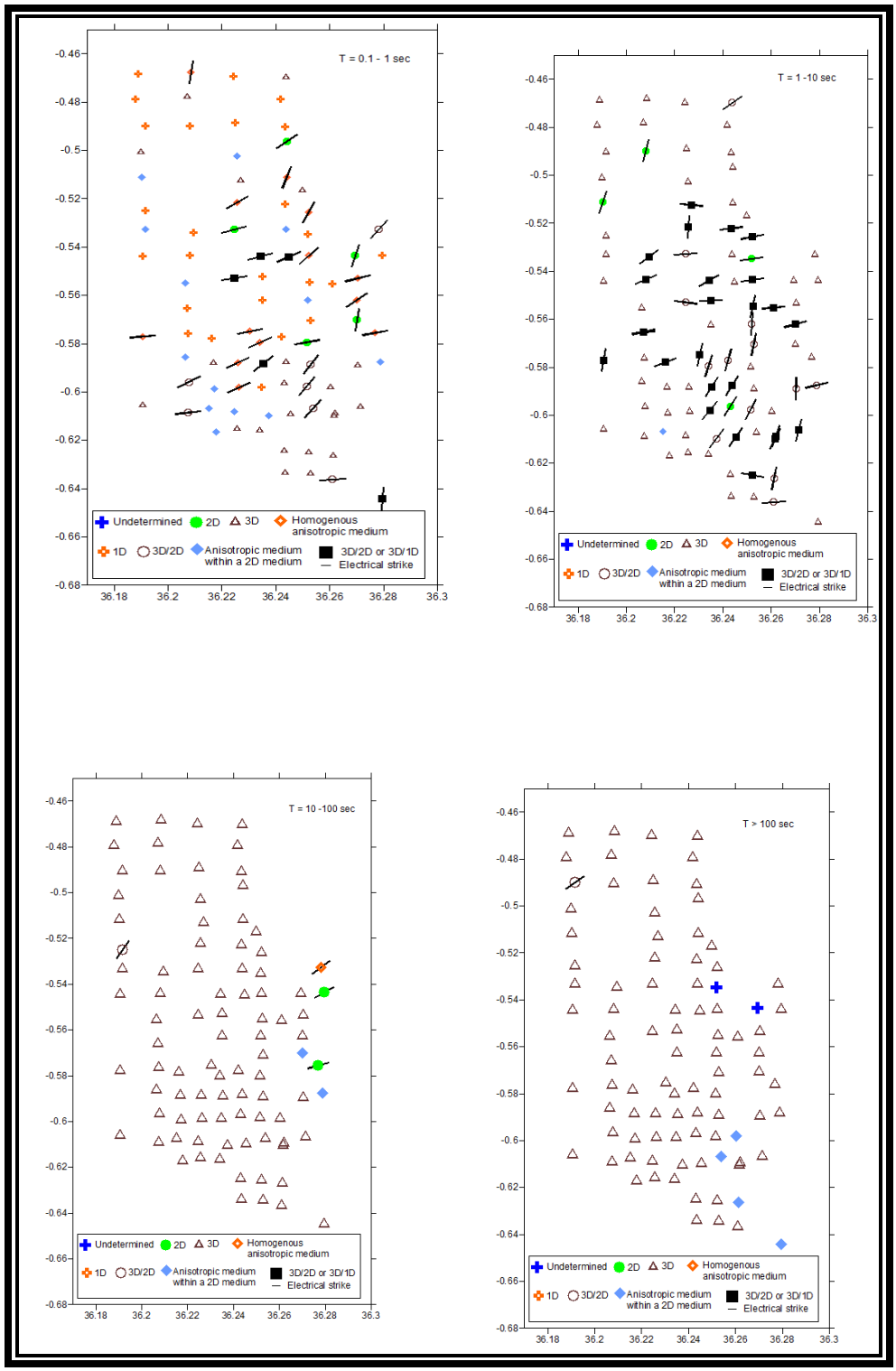

Figure 1.4: Eburru geothermal field and Badlands area.

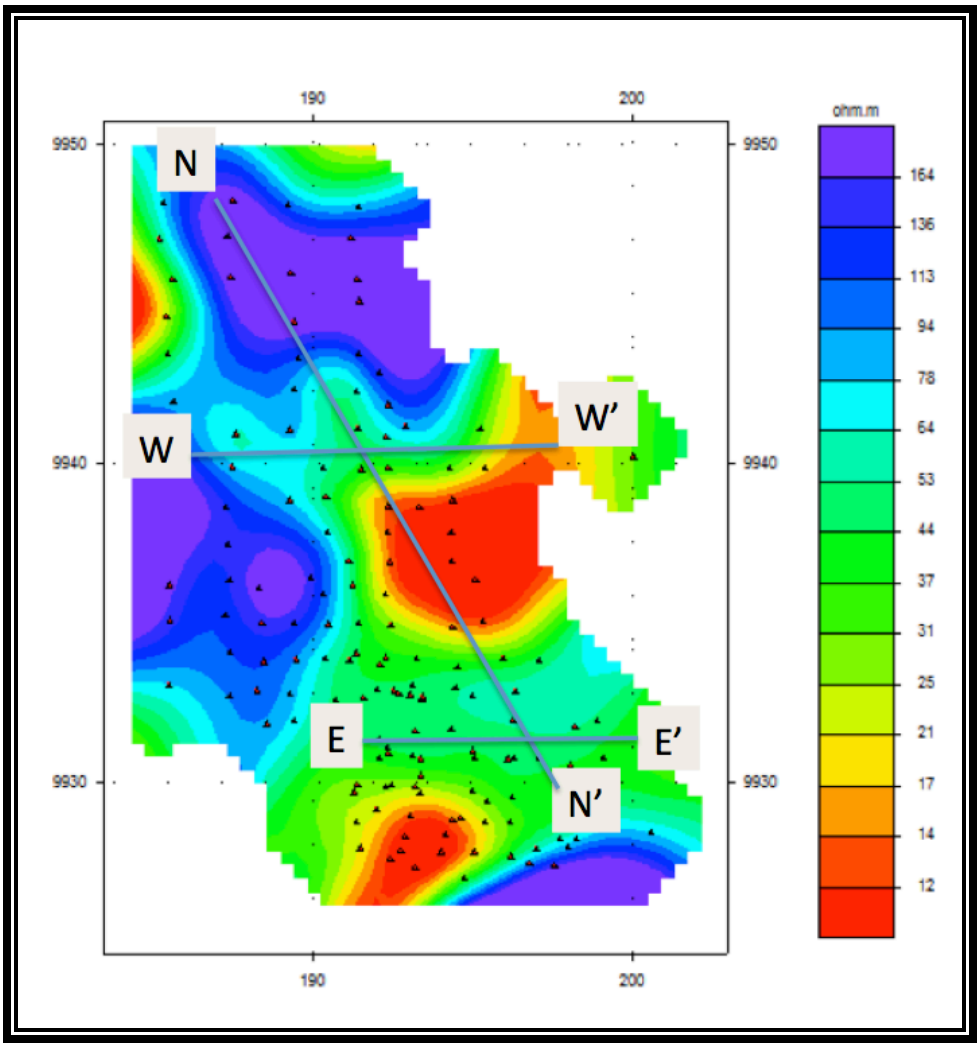

Figure 1.5: Resistivity depth slice at -2000m elevation derived from 1D inversion of MT data. The resistivity distribution with depth shows low resistivity anomalies in a northwest southeast orientation. 2D inversion was performed along the selected profiles. Little black triangles indicate location of MT sounding.

1.2.5 2-D Data inversion

2-D inversion of the data was done for both TE and TM curves using Randy Mackie subroutines (Rodi and Mackie, 2001). A forward model was calculated and used as a starting model. A total of 70 iterations were done for each profile to generate the final model and the root means square error was on average below 3% after the iterations.

1.3 Results

The results are shown as 2-D inversion profiles (Figures 1.6 – 1.8). Figure 1.6 shows an east-west 2-D profile of resistivity variation with depth. Low resistivity (LR1) anomaly (< 5 ohm-m) is a shallow anomaly, at 3.5km from the surface with a diameter of 1.5km. LR2 is a low resistivity anomaly dipping northwest. This body extends for 5km and may be connected to LR3 at depth. LR3 is the main intrusive body, < 4 ohm-m. We cannot resolve the lateral extent because we do not have data beyond the profile extent however we see it is oriented east west. High Resistivity (HR) zones are thick, about 3km thick and 10km wide while the edges are linear.

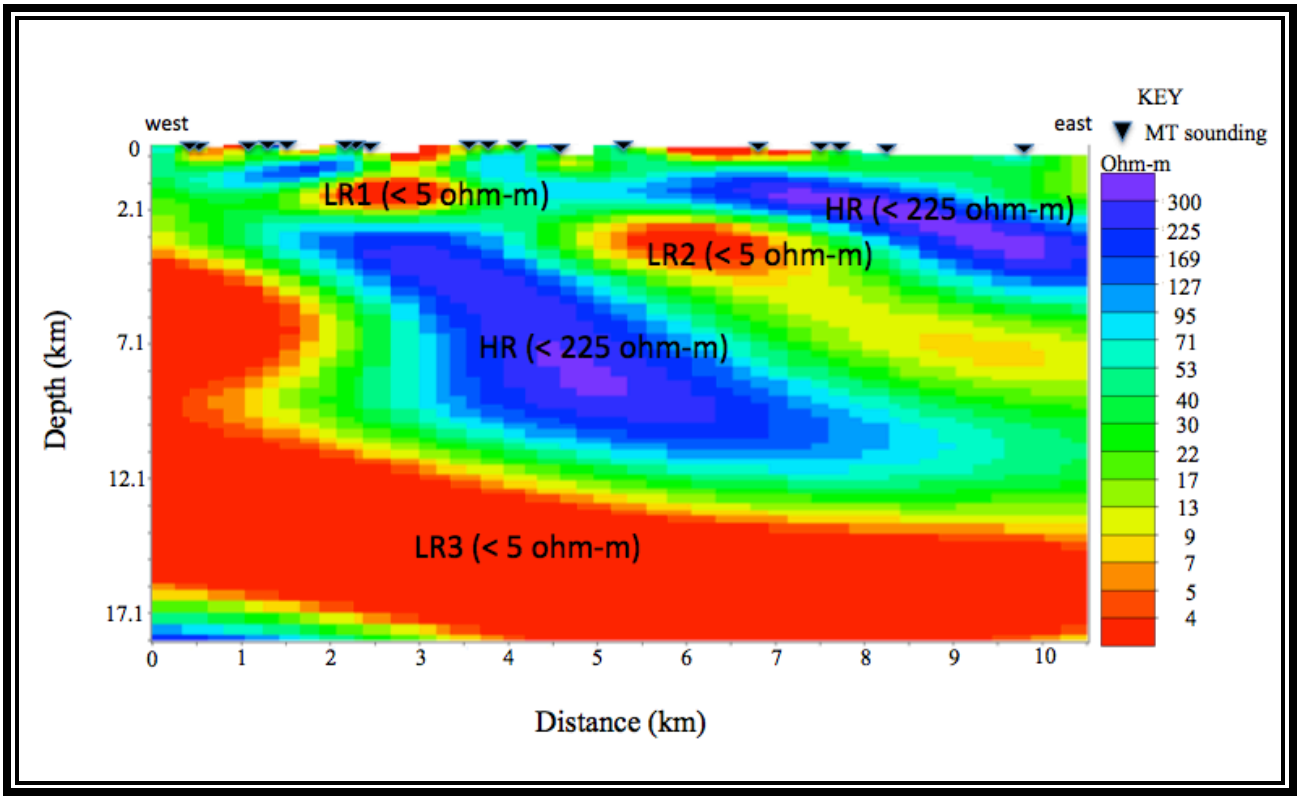

Figure 1.6: East-west 2D resistivity profile along Eburru crater crossing well 1.

Figure 1.7 shows an east-west profile along the Badlands area. The surface is characterized by a ~1km thick continuous low resistivity layer, LR1, near the surface. HR zone

occurs as two separated zones, a large zone towards the east and a thinned layer on the east side. HR on the west is ~2km deep is large (7km by 5km=35km^2) and it thinner closer to the surface. The HR zones have a characteristic thinning out towards east side. At 6km deep a LR3 zone is dominant and it extends to the center E direction. An intermediate zone below the HR is large and appears to be connected to the LR3.

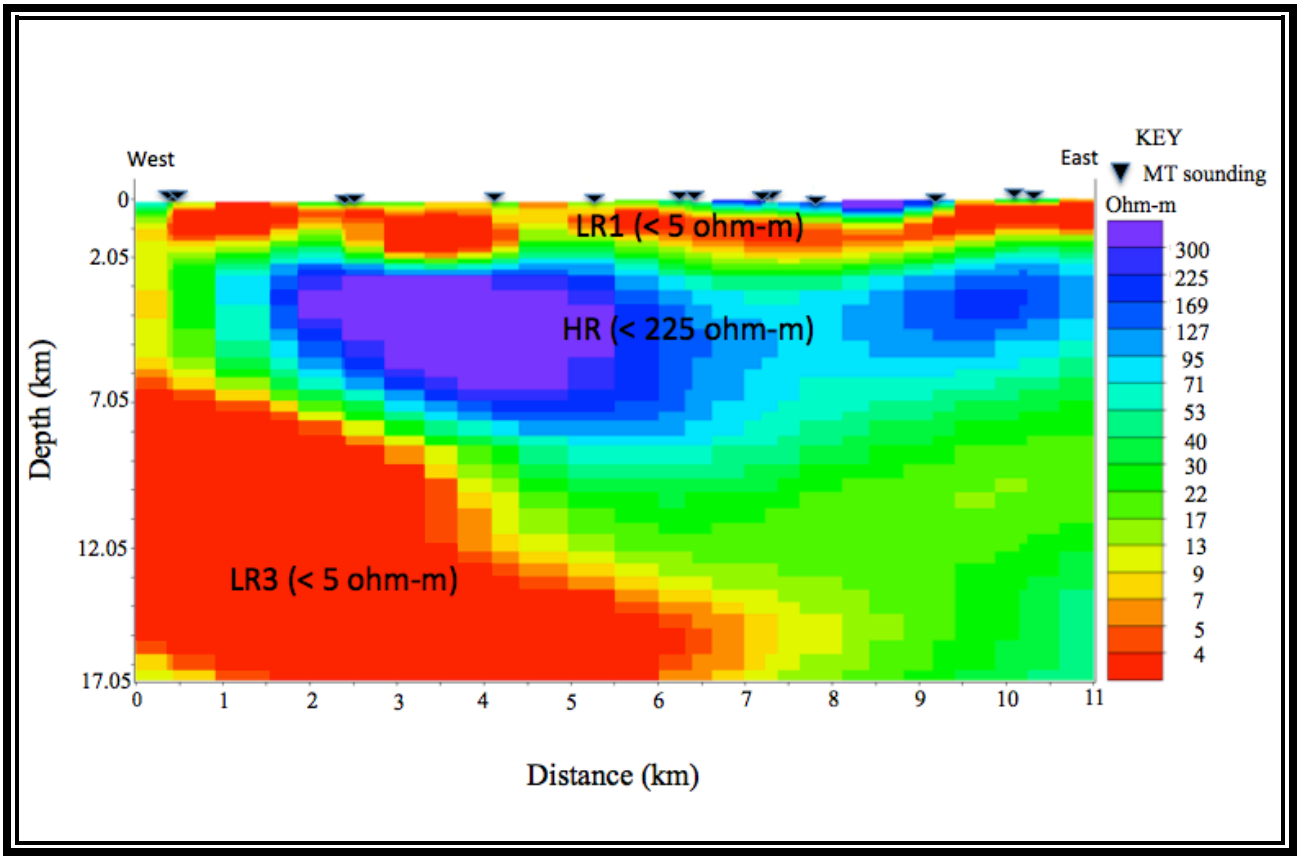

Figure 1.7: East-west 2-D profile along Badlands area, north of Eburru massif.

Figure 1.8 is a profile selected from Badlands (NW) to Eburru crater (SE). At the shallow surface thick layers LR1, ~2km thick, extends along the profile length. LR2, a shallow anomaly about 2km wide can be seen in the middle of the profile and a thick continuous HR confines it. At the contact zone with LR2 anomaly, the HR body seems thinned and takes the outline of the LR2. LR3 is a deep-seated body and it has two peaks, towards southwest (Eburru crater) the depth to its surface is ~6km and towards northwest it is ~9km. The length extent of LR3 is ~9km

and is seems to be extending on the northwest and southwest directions. Toward the end of the profile SE an edge of a LR zone can be seen however it is not well resolved.

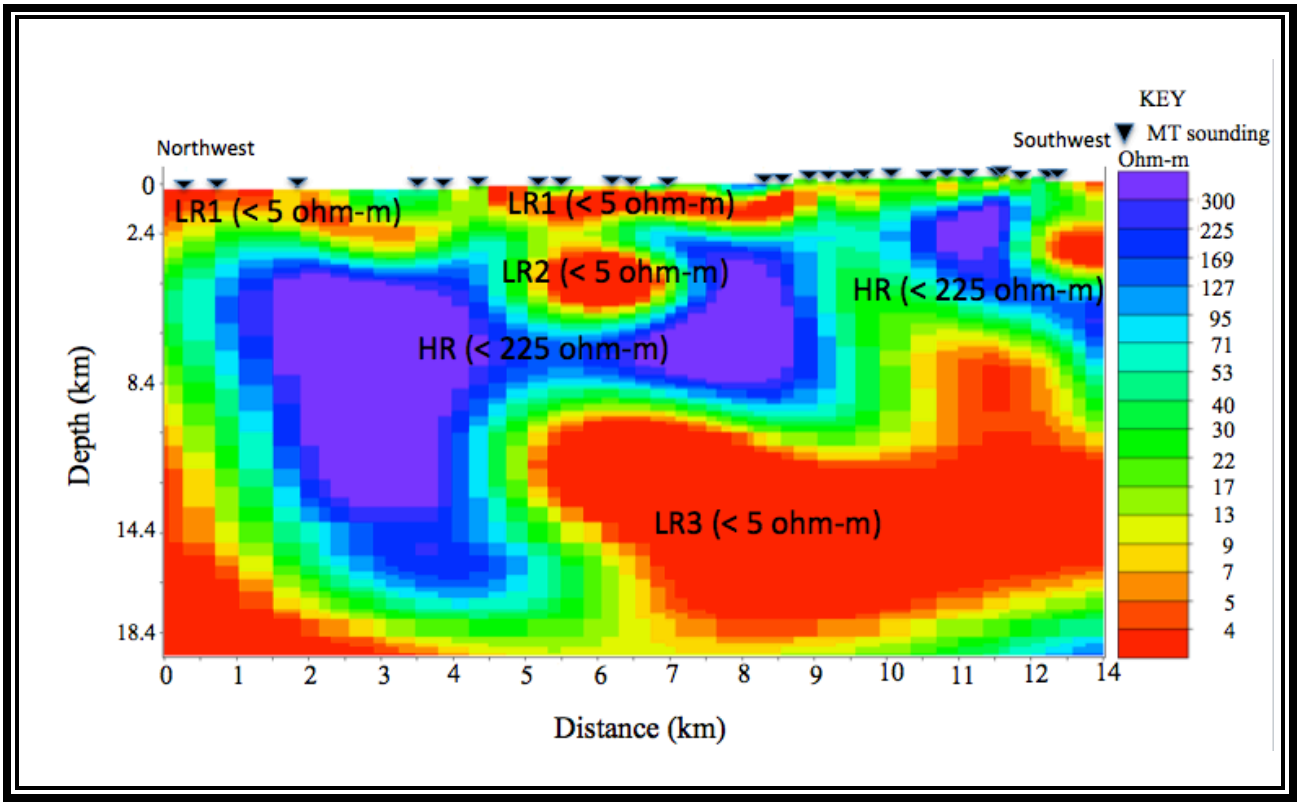

Figure 1.8: 2-D resistivity profile NW-SE starting at Badlands (NW) and Eburru (SE). A low resistivity structure is observed in the Badlands area.

1.4 Discussions

The 2-D resistivity results indicate an active geothermal field that has characteristics of a prolific high temperature system (Lichoro, 2009; Mwangi, 2013; Omiti, 2013; Wamalwa and Serpa, 2013). In general, the models show a low resistivity heat source, sometimes a high resistivity core around the heat source, and a high resistivity shallow surface geothermal cap rock. The signature is distinct because of the heat action on fluids and rocks causes dissolution and rock alteration where new hydrothermal minerals have different resistivity values (Flovenz et al., 1985; Pellerin et al., 1996, 1996) depending on the temperature regime which plays an important role in reducing resistivity.

The clays form at different temperatures and hence the mixed clay layer forms the high resistivity geothermal cap. Figure 1.9 shows a typical active geothermal system with hydrothermal products and the corresponding resistivity of the clay minerals. We use this model to interpret what we observe in Eburru and Badlands (Pellerin et al., 1996).

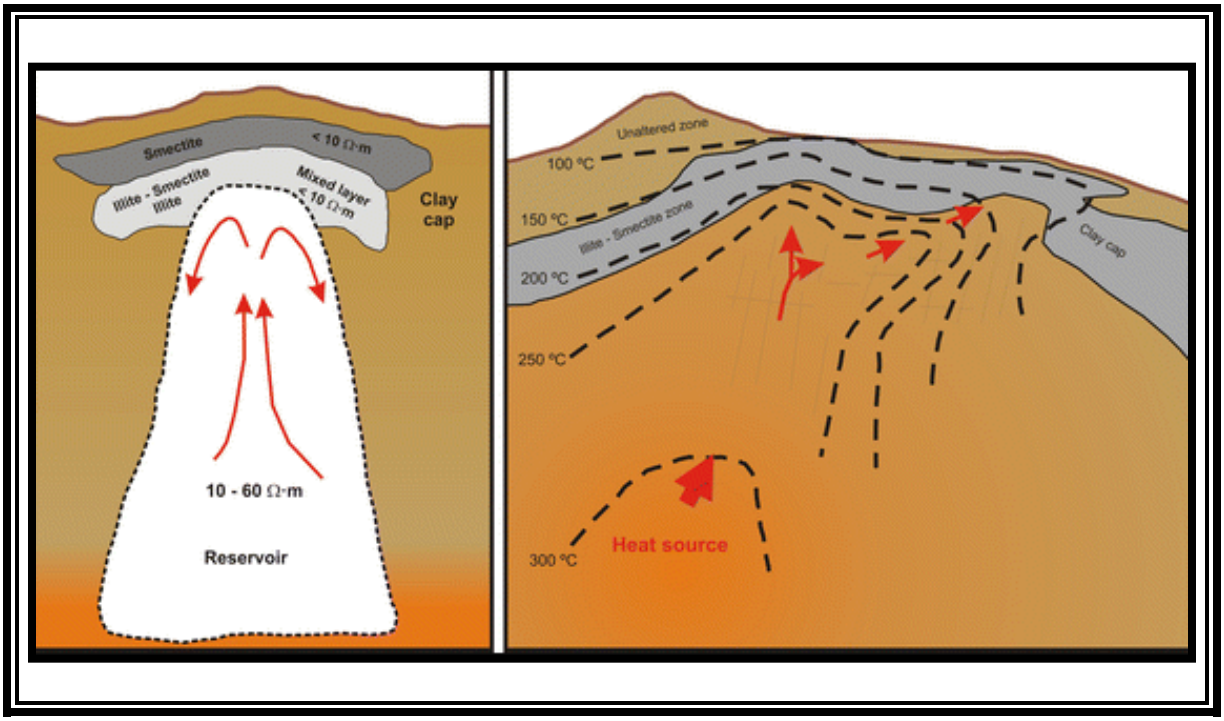

Figure 1.9: Geophysical signature and temperature regime in a geothermal set up (Adapted from (Pellerin et al., 1996; Cumming, 2009). The conductive clays occur close at the top of the reservoir.

Away from the heat source linear structures inferred to indicate faults are interpreted to be channels for fluid flow; i.e. meteoric water recharge is believed to circulate to great depths because of the depths of the various faults Figure 1.9. The high resistivity material is interpreted as the remnants of series of trachytic rocks extruded over time forming the volcano. The high resistivity is because it is thick, crystalline, and the wall rock interaction along contact zones with the intrusive block fluid flows.

Eburru is a massif with several volcanic eruption centers and the magnetotelluric data shows magma chambers are the source of the volcanism observed at the surface. The linear faults are oriented the same direction as the step rift faults (Figure 1). A shallow intrusion is interpreted to lie above the main intrusion and they appear to be connected. The shallow intrusion is interpreted to be the heat source for the well 1 reservoir. Toward the west side of the profile a larger and deeper heat source is observed but only the edge of it is mapped due to a lack of data coverage. It is interpreted to be a magma chamber for the Ol Donyo Eburru peak west of the main Eburru crater. Intrusions around main Eburru crater are observed to dip making them linear and we believe we are observing main rift step faulting.

At the surface a low resistivity geothermal cap is observed in all profile sections. This implies that there is a dynamic reservoir where geothermal fluids flow is depositing hydrothermal minerals as temperature decreases away from the heat source hence making a low resistivity layer (Pellerin et al., 1996), which is observed from the surface. The application of electromagnetics to understand the subsurface structures has proved to give crucial information about geothermal activity under the volcanoes.

1.5 Conclusion

The exploration wells in Eburru targeted structures expected to be the up flow zones in the geothermal system and were widely spaced to determine the extent of the resource. Those initial wells indicated Eburru has good geothermal potential but its development requires more subsurface information. Our EM study indicates the geothermal and volcanic activities in this region are structurally controlled. That is, magma and hydrothermal fluids flow up along major faults. This is consistent with the observation that fumaroles are aligned with regional fault strikes. The MT data indicate a number of east-dipping, linear zones separating regions of high resistivity from areas of low resistivity. We interpret those zones to correspond to faults that provide a pathway for fluid migration and separate magma from cooler rock.

A significant observation in this study is the presence of a nearly continuous low resistivity body below about 8 km depth in the region. This body is inferred to be the major magma reservoir associated with the formation of Eburru massif.

The LR3 anomalies indicate the deep heat sources and the origin is from the east. Because of the multiple craters in the region, it is difficult to identify all of the critical surface structures but the magma chamber appears to be deep, averaging approximately 10 km deep, with shallow volcanic activity focused near major faults. Because the inflow of cold meteoric water that appears to be recharging the system is also likely to use the same plumbing system we would expect to see temperature inversions in some wells at the depth where the two different water circulation systems intersect. This is consistent with the findings from the first exploration wells. It will be important in developing the geothermal potential of Eburru to consider both circulating systems when siting wells. The best places to put an exploration wells are the areas near shallow magma source such as LR2 as it is most likely they are supporting a geothermal system above it.

The high resistivity zones in Eburru relate to the crustal rocks that are actively being reworked and assimilated as seen by MT data (Figure 1.9). The magma bodies dominate the 8-12km depth and probably deeper. It is expected that through the process of crustal thinning the magma rising to the lower crust is assimilated and have the ultramafic mantle material warping up to the lower crust. Figure 1.10, summarizes the observations in this field and the connection to other volcanoes such as Olkaria, which show magma intrusion at depth an integration of seismic, gravity and electromagnetic methods.

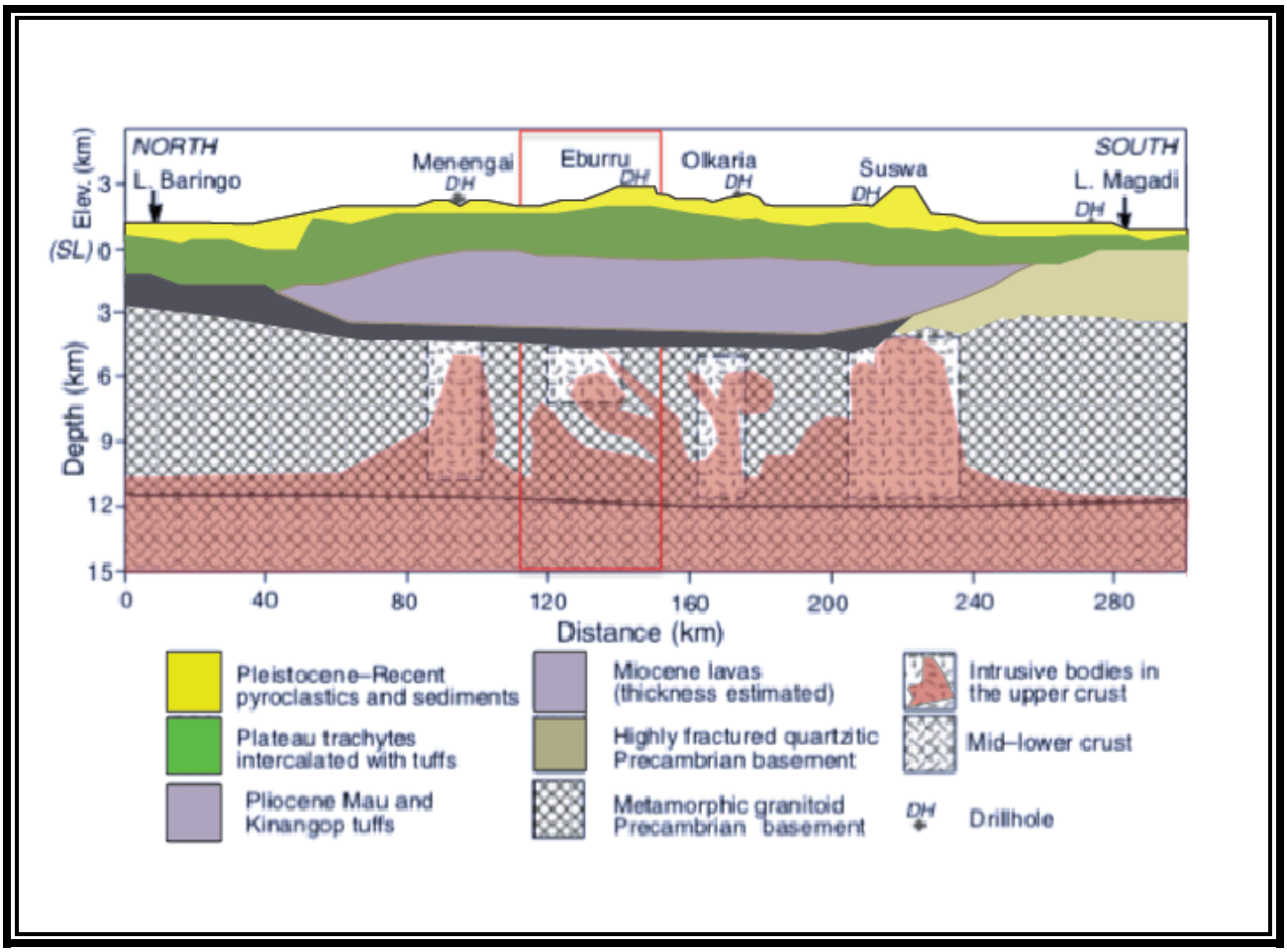

Figure 1.10: A modified geological model incorporating magnetotelluric data seismic, gravity and drill core information (Modified from Simiyu, (2000). Eburru and Badlands volcanic region is highlighted in the red box. This model shows crustal thinning by magma, which has been shown to be 8-12km below surface.

1.6 Acknowledgments

We would like to thank Kenya Electricity generating company (KenGen) for providing the data, facilitating travel and logistical support during fieldwork. We appreciate the Geophysicist Section staff at KenGen, for working tirelessly collecting data and more so for responding to queries regarding data. Thanks are due to University of Texas at El Paso where one of the authors, Anna Mwangi, was undertaking doctoral studies, for providing software/ hardware for analysis and assistantship throughout the length of the study.

1.7 References

Árnason, K., 2018, The Static Shift Problem in MT Soundings, https://pangea.stanford.edu/ERE/db/WGC/papers/WGC/2015/13031.pdf (accessed August 2018).

Arusei, M.K., 1991, HYDROCHEMISTRY OF OLKARIA AND EBURRU GEOTHERMAL FIElDS, KENYAN RIFT VALLEY: 2, 39 p.

Baker, B.H., Mohr, P.A., and Williams, L.A.J., 1972, Geology of the Eastern Rift System of Africa, *in* Geological Society of America Special Papers, Geological Society of America, v. 136, p. 1–68, doi:10.1130/SPE136-p1.

Baker, B.., and Wohlenberg, J., 1971, Structural evolution of the Kenyan Rift Valley: v. 229, 538–542 p.

Berdichevsky, M.N., and Dmitriev, V.I., 2008, Models and Methods of Magnetotellurics: Berlin, Heidelberg, Springer Berlin Heidelberg, doi:10.1007/978-3-540-77814-1.

Clarke, M.C.., Woodhall, D., and Darling, G., 1990, Geological, volcanological and hydrogeological controls on the occurrence of geothermal activity in the surrounding Lake Naivasha, Kenya: British Geological Survey, 138 p.

Cumming, W., 2009, Geothermal Resource Conceptual Models Using Surface Exploration Data:

Flovenz, O.G., Georgesson, L.., and Arnason, K., 1985, Resistivity Structure of the upper crust in Iceland: v. 90-B12, p. 10,136-10,150.

Gamble, T.D., Goubau, W.M., and Clarke, J., 1979, Magnetotellurics with a remote magnetic reference: GEOPHYSICS, v. 44, p. 53–68, doi:10.1190/1.1440923.

Gioncada, A., and Landi, P., 2010, The pre-eruptive volatile contents of recent basaltic and pantelleritic magmas at Pantelleria (Italy): Journal of Volcanology and Geothermal Research, v. 189, p. 191–201, doi:10.1016/j.jvolgeores.2009.11.006.

Lagat, J.K., 2003, Geology and the geothermal systems of the southern segment of the Kenya Rift, *in* Reykjavík, Iceland, http://www.jardhitafelag.is/media/PDF/S04Paper107.pdf (accessed May 2016).

Lichoro, C., 2009, JOINT 1-D INVERSION OF TEM AND MT DATA FROM OLKARIA DOMES GEOTHERMAL AREA, KENYA: United Nations University- Geothermal training Programme, 289–318 p., http://www.os.is/gogn/unu-gtp-report/UNU-GTP-2009-16.pdf (accessed May 2016).

Maguire, P.K.H., Swain, C.J., Masotti, R., and Khan, M.A., 1994, A crustal and uppermost mantle cross-sectional model of the Kenya Rift derived from seismic and gravity data: Tectonophysics, v. 236, p. 217–249, doi:10.1016/0040-1951(94)90178-3.

Martí, A., Queralt, P., and Ledo, J., 2009, WALDIM: A code for the dimensionality analysis of magnetotelluric data using the rotational invariants of the magnetotelluric tensor: Computers & Geosciences, v. 35, p. 2295–2303, doi:10.1016/j.cageo.2009.03.004.

Martí, A., Queralt, P., Ledo, J., and Farquharson, C., 2010, Dimensionality imprint of electrical anisotropy in magnetotelluric responses: Physics of the Earth and Planetary Interiors, v. 182, p. 139–151, doi:10.1016/j.pepi.2010.07.007.

McNeice, G.W., and Jones, A.G., 2001, Multisite, multifrequency tensor decomposition of magnetotelluric data: Geophysics, v. 66, p. 16.

Mwangi, A.W., 2013, JOINT 1D INVERSION OF MT AND TEM DATA FROM EBURRU, KENYA, AND PROCESSING OF GRAVITY DATA FROM THEISTAREYKIR, NE-ICELAND: United Nations University- Geothermal training Programme 27, http://www.os.is/gogn/unu-gtp-report/UNU-GTP-2011-27-1.pdf (accessed May 2016).

Omiti, A., 2013, RESISTIVITY STRUCTURE OF THE EBURRU GEOTHERMAL FIELD, KENYA, DEPICTED THROUGH 1D JOINT INVERSION OF MT AND TEM DATA: United Nations University- Geothermal training Programme, 599–624 p., http://os.is/gogn/unu-gtp-report/UNU-GTP-2014-05.pdf (accessed May 2016).

Pellerin, L., Johnston, J., and Hohmann, G., 1996, A numerical evaluation of electromagnetic methods in geothermal exploration: GEOPHYSICS, v. 61, p. 121–130, doi:10.1190/1.1443931.

Rodi, W., and Mackie, R., 2001, Nonlinear conjugate gradients algorithm for 2-D magnetotelluric inversion: GEOPHYSICS, v. 66, p. 174–187, doi:10.1190/1.1444893.

Scaillet, B., 2001, Phase Relations of Peralkaline Silicic Magmas and Petrogenetic Implications: Journal of Petrology, v. 42, p. 825–845, doi:10.1093/petrology/42.4.825.

Simiyu, S.M., 2000, An integrated geophysical analysis of the upper crust of the southern Kenya rift: Geophys. J. Int, v. 147, p. 543–561.

Simiyu, S.M., 1990, The Gravity Structure of Eburru, Kenya: United Nations University-Geothermal training Programme The Gravity Structure of Eburru, Kenya 13, https://orkustofnun.is/gogn/unu-gtp-report/UNU-GTP-1990-13.pdf (accessed October 2018).

Simiyu, S.M., and Keller, G.R., 2001a, An integrated geophysical analysis of the upper crust of the southern Kenya rift: Geophysical Journal International, v. 147, p. 543–561, doi:10.1046/j.0956-540x.2001.01542.x.

Simiyu, S.M., and Keller, G.R., 2001b, An integrated geophysical analysis of the upper crust of the southern Kenya rift: Geophysical Journal International, v. 147, p. 543–561, doi:10.1046/j.0956-540x.2001.01542.x.

Stephen, J., Gokarn, S.G., Manoj, C., and Singh, S.B., 2003, Effects of galvanic distortions on magnetotelluric data: Interpretation and its correction using deep electrical data: Journal of Earth System Science, v. 112, p. 27–36, doi:10.1007/BF02710041.

Wamalwa, A.M., and Serpa, L.F., 2013, The investigation of the geothermal potential at the Silali volcano, Northern Kenya Rift, using electromagnetic data: Geothermics, v. 47, p. 89–96, doi:10.1016/j.geothermics.2013.02.001.

Wetang'ula, G.N., 2012, GEOTHERMAL ENERGY DEVELOPMENT & POTENTIAL, BIODIVERSITY CONSERVATION AND TOURISM DEVELOPMENT: EXAMPLES FROM KENYA: , p. 12.

Chapter 2: Characterization of the geothermal system of the Mt. Longonot Volcano and Olkaria Domes volcanic field, Kenyan Rift System

Abstract

The central Kenyan rift floor has a chain of volcanoes that are geothermal fields or promising geothermal prospects waiting to be developed. The most successful geothermal field along the East Africa rift is Olkaria geothermal system, the biggest geothermal field in Africa, is part of the central rift volcanoes. It is adjacent to the Mt Longonot strato volcano on its east side. Mt Longonot has a large magma system, which rises as a diapir to just 3km below the crater surface. Magnetotelluric data indicate the magma system is connected to the Olkaria ring of Domes at approximately 10 km depth. The Mt Longonot magma heat sources occur below the volcano but are also upwelling toward the eastern flank of the volcano. The shallow conductive cap rock at depths of 800m below surface indicates an active geothermal system depositing conductive clays as a marker of decreasing temperature away from the localized heat sources.

2.1 Introduction

To grow its economy, Kenya is working to increase its energy production and support its development agenda. A major focus of this work is to exploit available geothermal resources within the Kenyan rift to replicate the success of the Olkaria geothermal field, which produces 687.5 Mwe. Adjacent to the Olkaria geothermal field (Figure 2.1) is the Mt Longonot volcano, and the separation between the volcanoes outer calderas is 3km. Due to their close proximity we would like to understand the magma systems beneath the two active volcanoes. Olkaria volcanic field has no clear outline of the caldera and this is in contrast to Mt Longonot which has an outer caldera and a central crater.

Mt Longonot is a Quaternary stratovolcano located approximately 10 km from the Olkaria geothermal field. Mt Longonot's recent eruptive history is similar to that of Olkaria and, for that reason, it is considered to have good geothermal potential. Thus, we undertook this

study to better understand the geologic character of the Longonot volcano and possibly the connection to the Olkaria volcanic field.

To achieve our goals we used electromagnetic methods. Those studies show a distinct connection between Olkaria and Longonot with an apparent shared deep (~10 km deep) magma source connecting the two geothermal prospects. There is strong evidence of a vertically rising magma diapir beneath Longonot and smaller, east-dipping diapirs beneath Olkaria to further suggest Longonot may be a good source of geothermal energy but also poses a volcanic hazard to the region. The development of the geothermal systems for the two volcanoes is dependent on the location of the up-flow zones and the heat regime in the shallow subsurface. This study gives insight into the optimization of the geothermal resources and management of both geothermal fields.

Figure 2.1: Location map of the Mt Longonot and Olkaria Domes within Kenya Rift valley. (DEM sourced from www.opentopography.org)

2.1.1 Previous work

Magnetotelluric (MT) data were collected in 2004 to investigate the reservoir system under Mt Longonot (Onacha, 2006) facilitated by Kenya Electricity Generating (KenGen) company. The area was explored using the gravity method by Geotemica Italiana in 1989 and detailed density contrasts due to lava and pyroclastic materials. Onacha (2006) performed a 2D inversion of the MT data and proposed a geothermal exploration well in the southern sector of the volcano.

2.1.1 Olkaria geothermal field

The Olkaria geothermal field has been successful in generating power for Kenya and is the second largest source of energy in the country. The major reason for the success is that Olkaria is an active volcanic field with the last eruption dated at approximately 250+100 years ago (Clarke et al., 1990). Olkaria has shallow magma bodies, estimated to be within 6 km of the surface, that provide heat sources to turn ground water into steam which is stored in interconnected porous reservoir rock that can be accessed though drilling. Pressurized steam is channeled to a power plant to turn a turbine making kinetic energy in the form of electricity. When the steam cools in the power plant it is re-injected into the ground to recharge the system. A variety of geophysical methods have been utilized in the Olkaria field to identify sources of heat, the locations of steam conduits, and the ideal locations to re-inject cooled water so that it will not cool the steam conduits but will be reheated and recycled through the system when needed.

Despite Olkaria's success as an energy provider, there is continued research into methods to improve the development of the field. In addition, the geothermal field also includes the Hell's Gate National Park where tourists visit to see the natural beauty and array of animals without the distraction of a major power plant. KenGen has worked to maintain the tourist attraction of the region and enhance the nearby communities in a variety of ways. Any additional development in the region would be expected to follow be similar to the Olkaria field and, thus, management of the geothermal resources is a very important concern.

2.1.2 Longonot geothermal prospect

Mt Longonot is located within approximately 10 km of Olkaria and, like Olkaria, it includes a National Park, the Longonot Park which is a major tourist attraction. Longonot has a very active volcanic history including the most recent eruption approximately 190 years ago. Scott, (1980) details a series of eruptions of peralkaline trachyte forming the flanks of the mountain in the late Pleistocene period. A caldera collapse episode occurred in the early Holocene followed by the eruption of voluminous pyroclastic material that was deposited around the volcano. Strong eruptions created an approximately 1.8 km diameter crater on Longonot and deposited hawaiite type trachyte lava flows. The youngest flow is composed of peralkaline trachyte. Volcanic ash and pumice rocks from Mt Longonot cover a large area around Longonot and also blanket most of the Olkaria volcanic field (Clarke et al., 1990; Muchemi, 1999). The nearby shield volcano, Mt. Suswa, has evidence of fractionation and magma mixing evidenced by anorthoclase zoning and magma mixing (White et al., 2012) and Longonot also has a history of basalts and trachytes lavas .

2.2 Magnetotelluric (MT) method

The MT method discovered by Tikhonov, (1950) and Cagniard, (1953) is a powerful tool for exploration of the subsurface resources such as oil and gas, mineral and geothermal exploration. It has been applied to explore many geothermal fields in various geological settings around the world e.g. Krusuvik geothermal field in Iceland (Hersir et al., 2015), Tendaho geothermal field in Ethiopia (Lemma Didana et al., 2013) and Coso geothermal field in the USA (Wamalwa et al., 2013b) . The method utilizes natural sources of electromagnetic waves that reach the earth's surface where they are absorbed by the earth. The waves are assumed to be plane waves that penetrate the earth's subsurface where the wave attenuates at depth based on the wavelength. The mode of attenuation is perpendicular to the earth's surface because material difference of air and the earth's surface. The MT method is very suitable for geothermal exploration because it can show the resistivity distribution with depth determined by the rock properties, fluid content or igneous activity (Berdichevsky and Dmitriev, 2008). The target depth

is determined by the length of recording of the time series MT data and also the ground properties such as resistivity of the general subsurface, permeability and period of the wave (Menezes, 2010).

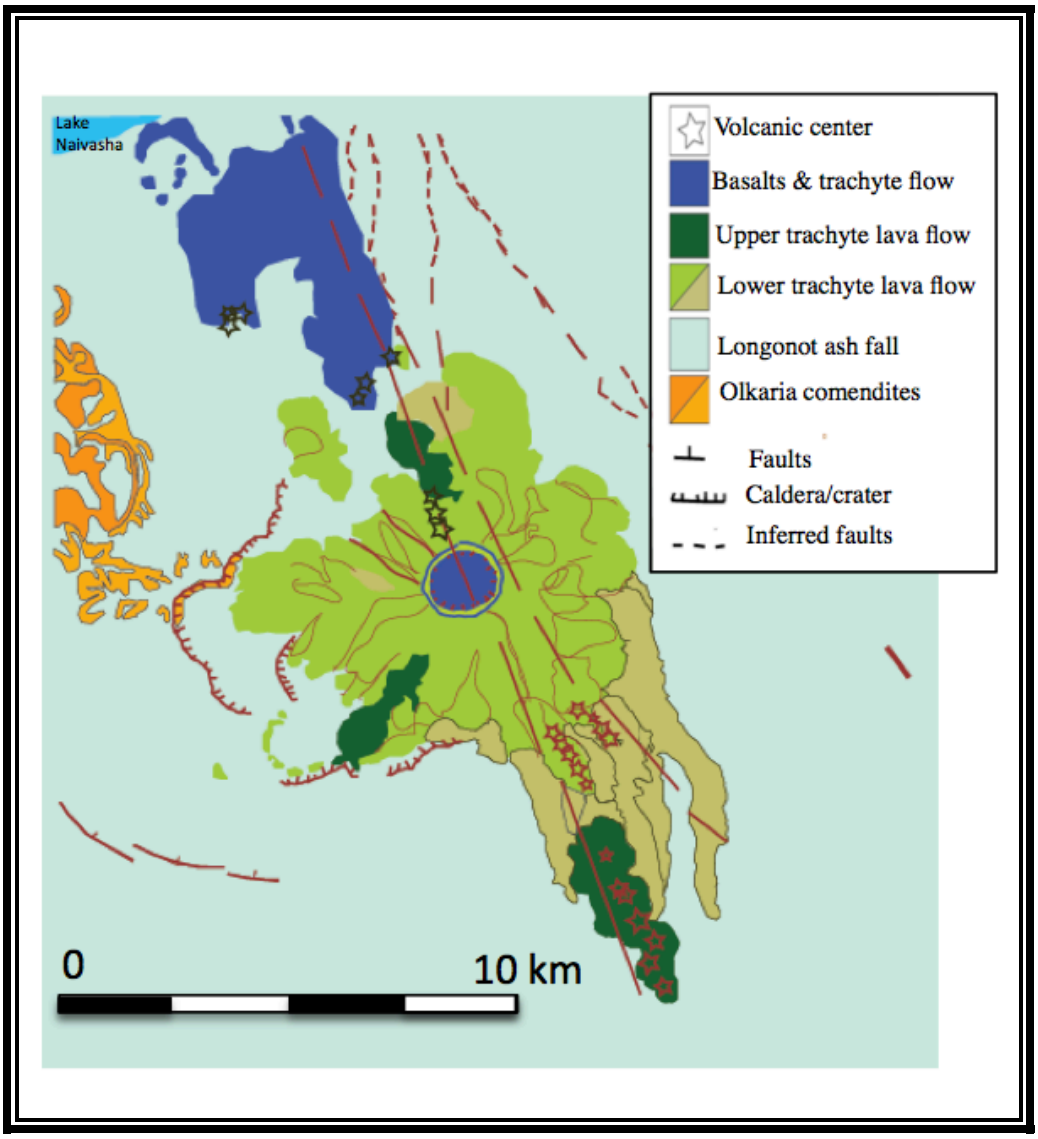

Figure 2.1b: Geological map of Mt Longonot and part of Olkaria Domes. The major faults observed are a fracture zone referred to as the Tecto volcanic axis.

2.2.1 Data Processing

We used MT data from the Olkaria Domes region and the 2004 data from Longonot collected by Onacha (2006) to perform dimensionality analysis and more importantly to explore the area between the Olkaria Domes and Mt Longonot in order to compare the two volcanic systems. The Mt Longonot data were provided to us in Electronic Data Interchange (EDI) format by KenGen and were already Fourier transformed and processed using Phoenix Geophysics™ software. We edited the EDI data to remove outliers using Winglink™ software. The processed transient electromagnetic data were used to correct the MT data for static shift and 1D inversion was done on each of the soundings.

2.2.2 Dimensionality

The electromagnetic signals penetrate the earth and long period waves travel deeper than short period waves because of attenuation. The ratio of the electric and magnetic waves, described as the impedance tensor, will contain information about the conductivity variation and whether it is 1D, 2D or 3D (Martí et al., 2009). To determine the dimensionality we used WALDIM code by Martí et al., (2009).

Data from Mt Longonot (figure 2.2) show dimensionality to be mainly 1D and 2D for short periods of 0.1-1 second. However, as the period increases from 1->100seconds a 3D trend becomes dominate. The electrical strike shows the direction of the conductivity, which is lined up along structures where fluids flow and, thus, there is a higher concentration of conductors. The strike direction for the Olkaria Domes and Longonot region is mostly east-west and northeast-southwest directed.

2.2.2 Geophysical modeling

To have a preliminary view of the resistivity variation, we made 1D resistivity depth slice at -2000m elevation using 1D-inverted soundings (Figure 2.3). The slice shows very low resistivity on the southeast side of the volcano and the area near Olkaria Domes. Seven profiles from the depth slices are used to perform 2D inversion and the results are shown figure 2.3. The

regional strike values used were determined using the tensor decomposition code by McNeice and Jones, (2001).

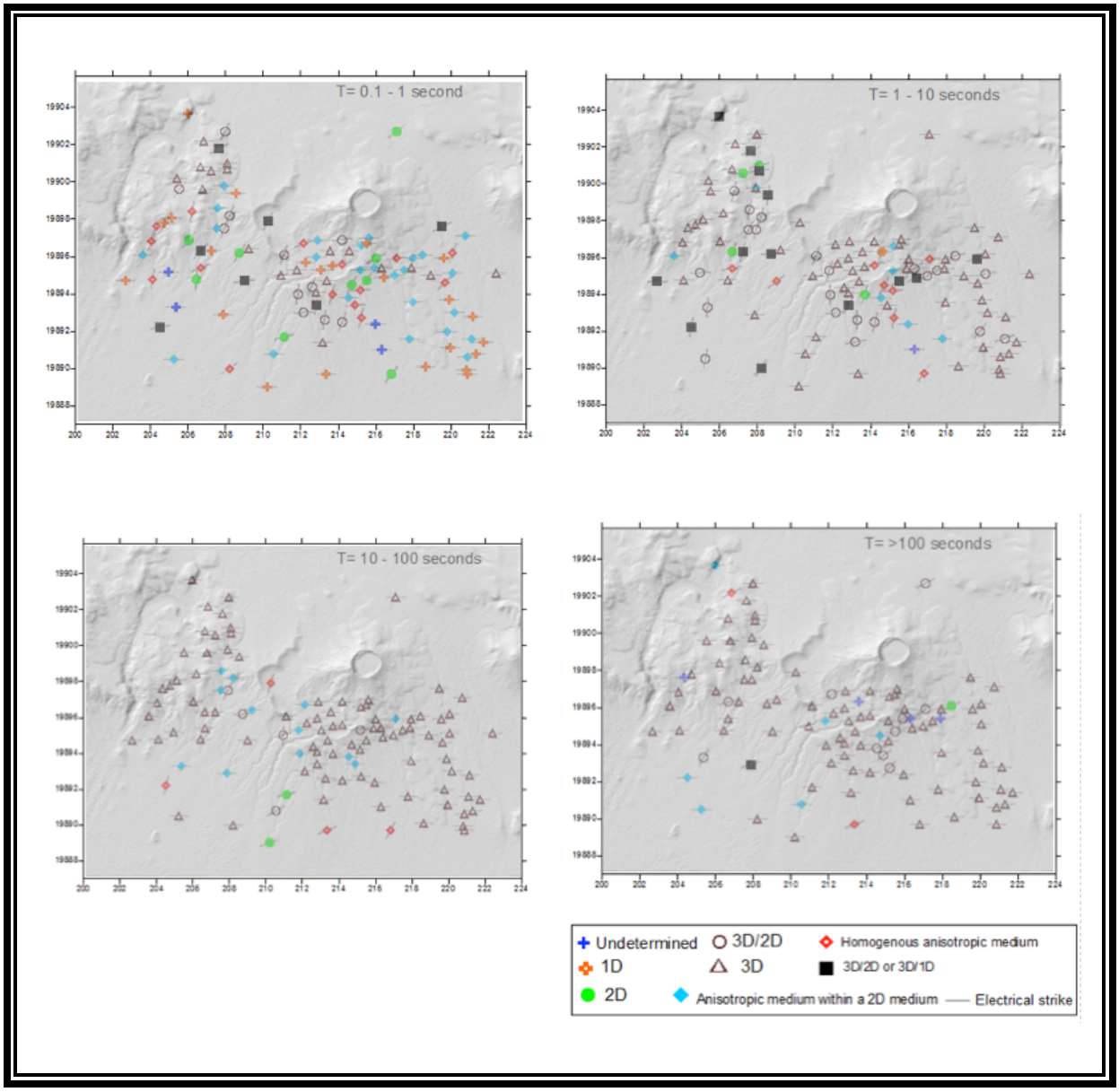

Figure 2.2: Dimensionality of Mt. Longonot and Olkaria Domes volcanoes.

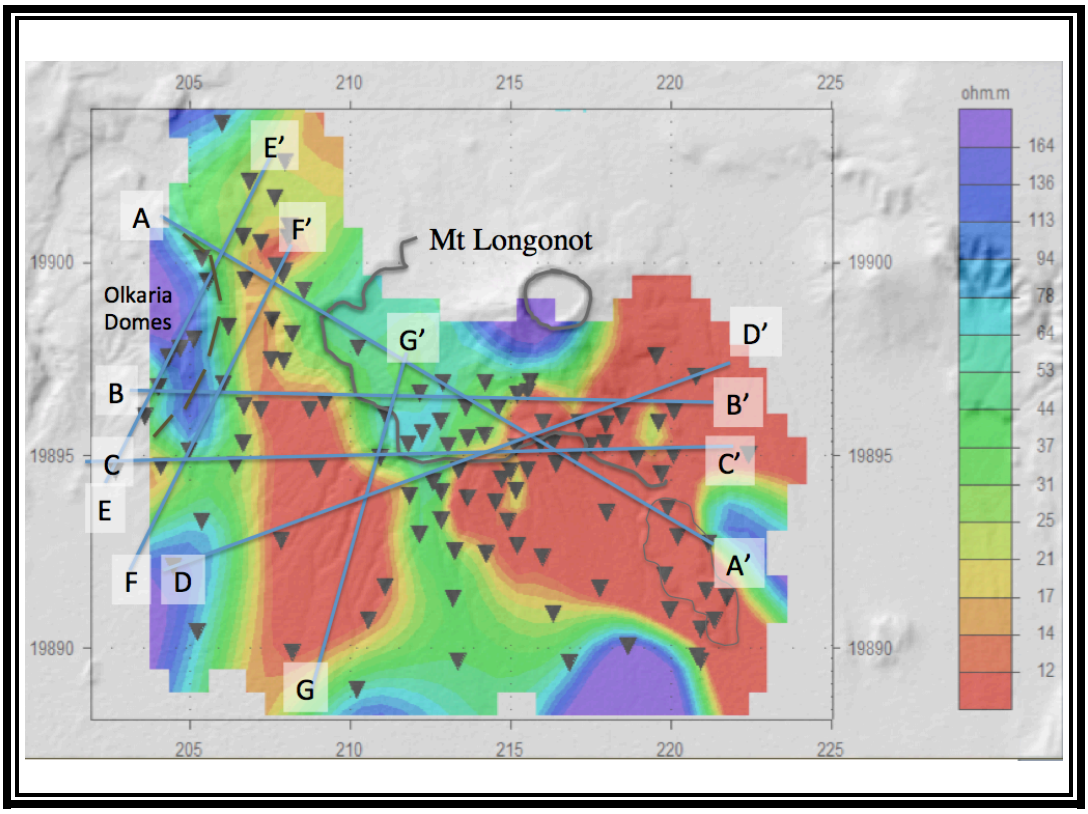

Figure 2.3: 1D resistivity slice at -2000m elevation showing low resistivity anomalies at the eastern flank of Longonot and to the west of Longonot outer caldera. Line profiles (A-G) were selected and 2D inversion performed; black triangles are the MT data locations.

2.3 Results

To image the Longonot prospect and the Olkaria Domes field we performed 2D inversion of the MT data. The results give high-resolution imaging (mapping an average depth of 18km) showing resistivity variation with depth and distance. The profiles are discussed below.

2.3.1 Profile A-A'

Figure 2.4 shows northwest-southeast profile shows LR1 is only thick where it is overlying LRZ2 in the southeast side. It is thin in the northwest and not pronounced. The HRZ blocks are more continuous and thick in the northwest side about 6km thick with the only interruption near the southeast region where LRZ2 is rising to 2.5km depth. LRZ2 anomaly is thinner than observed in other profiles in the northwest sections. LRZ3 is shallower where its base is 12 km deep to the low resistivity zone.

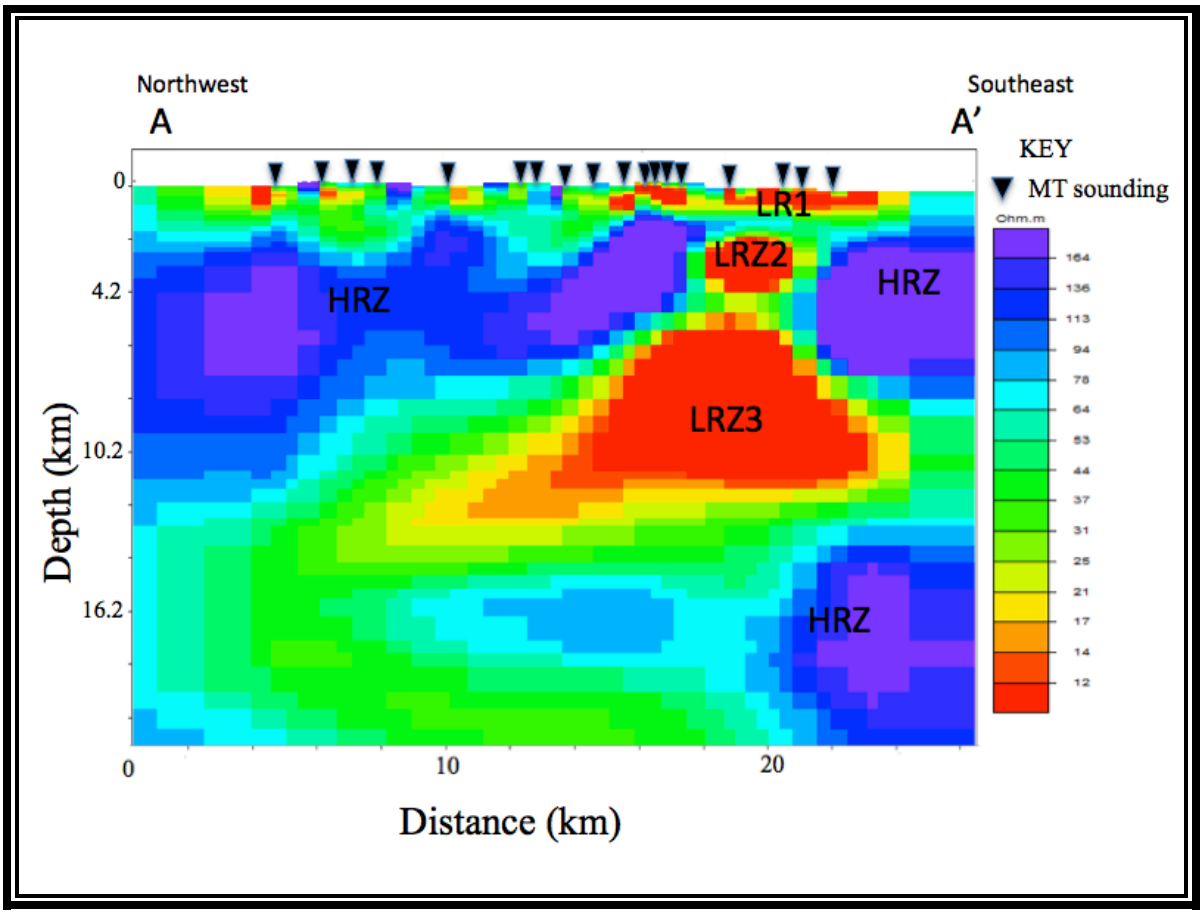

Figure 2.4: Profile A-A'- 2D inversion resistivity profile northwest area south of Olkaria Domes to northeast side of Longonot.

2.3.2 Profile B-B'

Profile B-B' (Figure 2.5) shows a thick low resistivity layer (LR1) at about 800m overlying a high resistivity zone (HRZ) that is thick and appears to separate low resistivity zones at depth. In this profile HRZ blocks are separated by very low resistivity anomalies LRZ2a that rises vertically below LR1 while LRZ2b branches to the east. To the west another HRZ separates the Olkaria Domes from the larger Longonot side. An inclined, intermediate resistivity zone appears to separate two HRZ blocks and connect LRZ3 with LR1 on the western side of the

profile. LR1 at the region below the intermediate zone is deeper than at other places along the profile. The base of LRZ3 is at 11km depth.

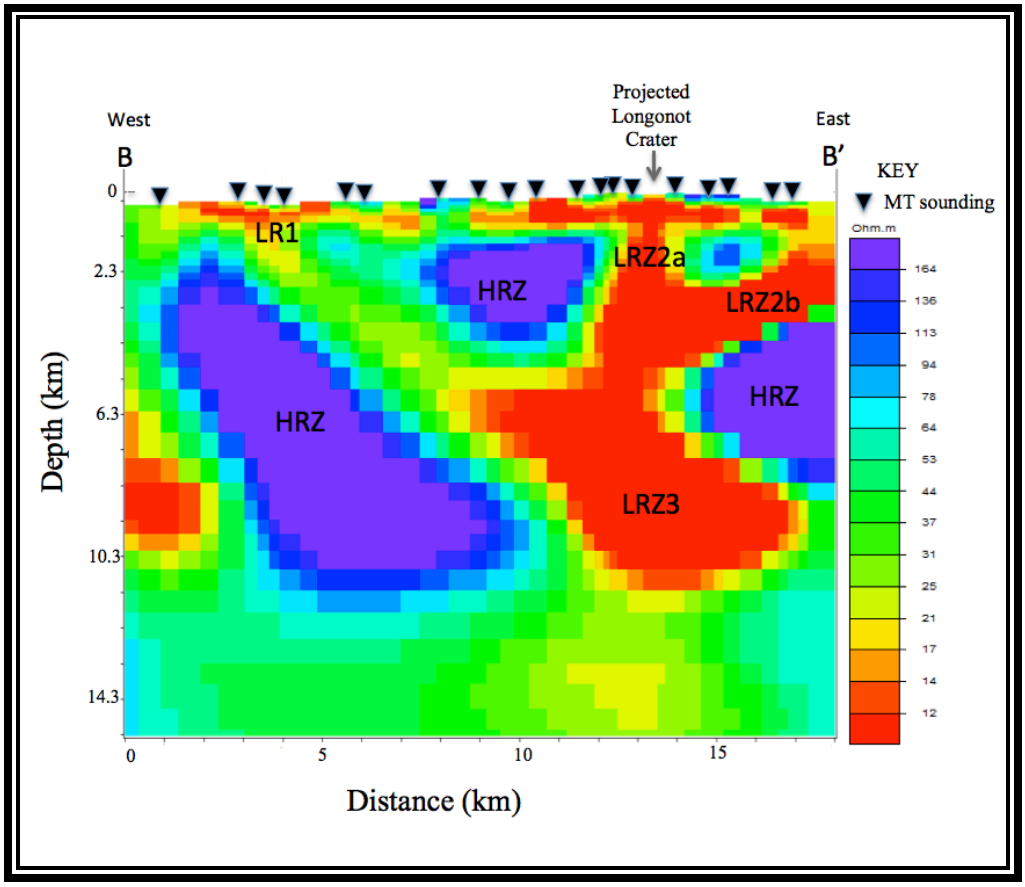

Figure 2.5: Profile B-B', Olkaria Domes (west) - Longonot (east) 2D inversion resistivity profile.

2.3.3 Profile C-C'

Profile C-C' (Figure 2.6) is parallel to profile B-B' (Figure 2.5) and they both cover the boundary between the Olkaria Domes and the Longonot region. Similar to profile B-B', a low resistivity zone at the upper surface, labeled LR1, has a thickness of about 800m beginning from the ground surface. The layer is present almost the entire length of the profile. At about 2.2 km depth, below LR1, is a thick, dipping high resistivity layer (HRZ) separated by a thick low resistivity zone (LRZ3) that rises from 10 km to approximately 3km (LRZ2) below ground

surface. HRZ block on the east side is thicker and deeper than the one on the west side. LRZ3 is horizontal at 10km depth and extends beyond the profile C-C' on both east and west directions. The depth to the base of LRZ3 is 15.5km on the west side and 19.5km on the east side.

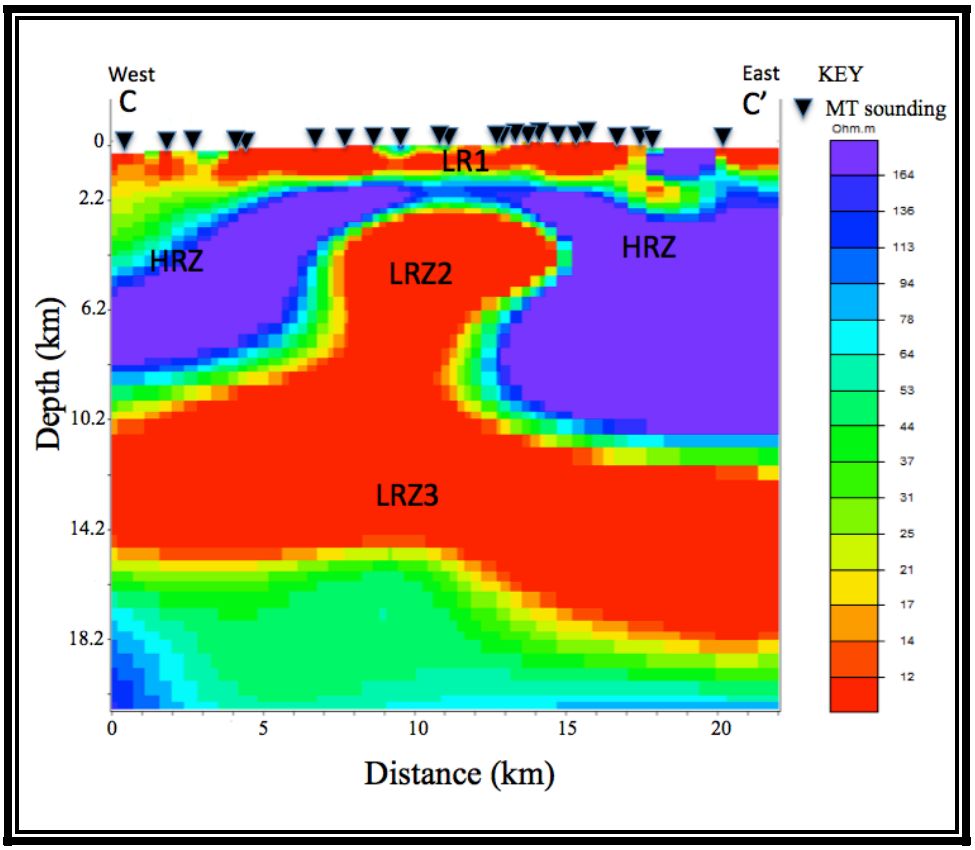

Figure 2.6: Profile C-C', Olkaria Domes (west) - Longonot (east) 2D inversion resistivity profile.

2.3.4 Profile D-D'

D-D' profile (Figure 2.7) shows low resistivity layer, LR1, ~800m thick at the upper surface. Underlying HRZ blocks dip to the southwest and are adjacent to LR2. Between the two high resistivity anomalies is an intermediate resistivity layer. The HR block (12km long and 8km thick) on the northeast extends beyond the profile length to the southwest and its top appears fractured at about 1km depth. LR3 anomaly is almost horizontal and the HR block adjacent at ~14km depth marks the northeast bound however to the southwest, it extends beyond the profile

length. We projected the Longonot crater at the edge of the profile. The depth to the base of LR3 is 18.3km.

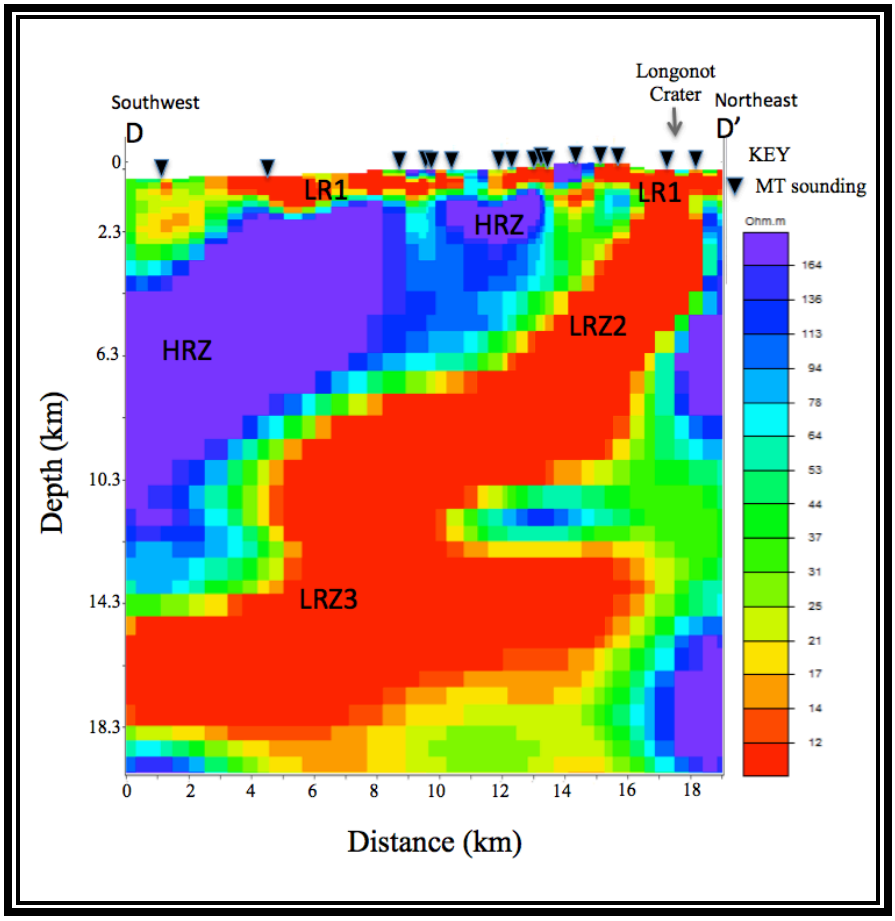

Figure 2.7: Profile D-D'- 2D inversion resistivity profile southwest, area south of Olkaria Domes to northeast side of Longonot.

2.3.5 Profile EE', FF' and GG'

These are 3 profiles parallel to each other and run roughly north to south. Their selection aims to image the boundary conditions between Olkaria Domes and Longonot in an east west direction.

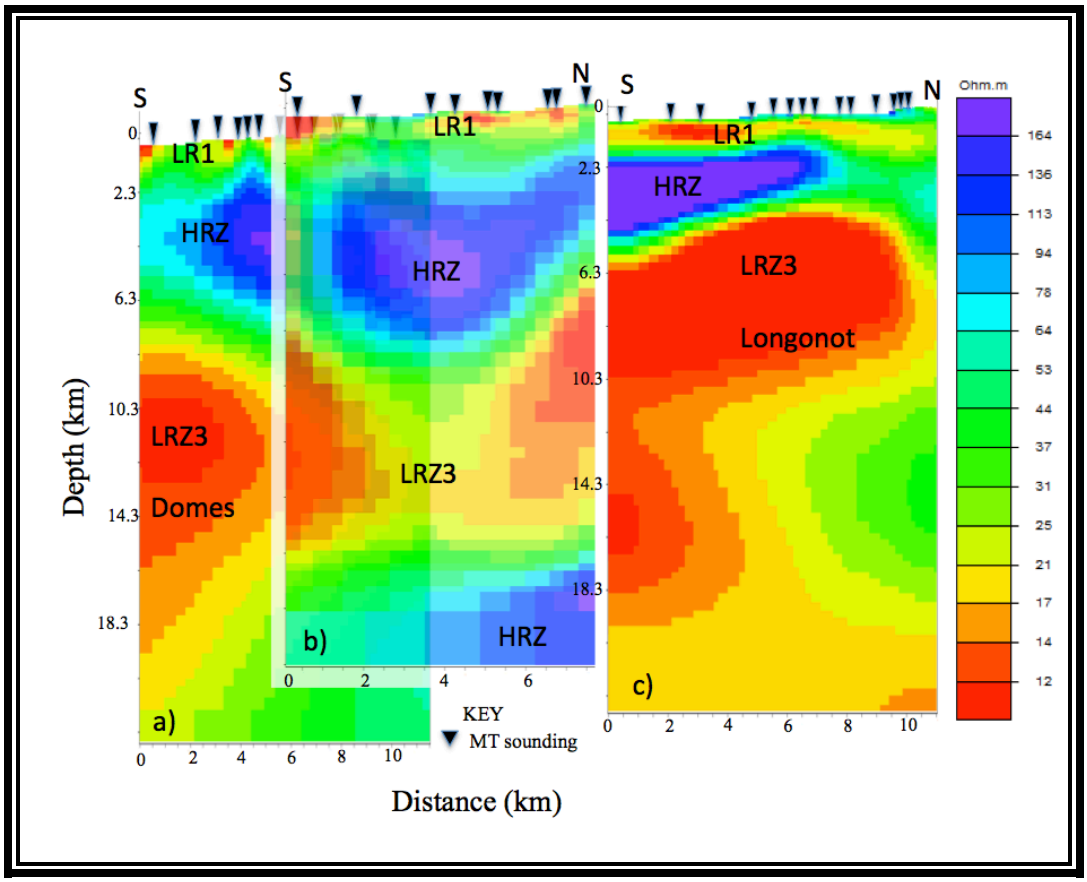

Figure 2.8: 2D inversion showing 3 parallel profiles from south to north 2.8a) profile E-E' 2.8b) profile F-F' and 2.8c) profile G-G'

Profile E-E' (2.8a) is located in the Olkaria Domes. Profile F-F' (2.8b) is in the region between the two volcanoes and profile G-G' (2.8c) is mainly on the Longonot side. All the profiles show consistency continuation features from the west to east. The profiles image LR1 which is quite thin in E-E' and thicker in Longonot. HRZ is thicker in F-F' than in Longonot.

Because the profiles oriented north south we are able to observe the connection of the low resistivity anomaly LR3Z anomaly between Olkaria Domes (Figure 2.8a) and Longonot (Figure 2.8c) is mainly through north south structure. LR3 in all profiles are connected at 10km. However, in Longonot LR3 rises to within 3km below surface. The morphology of the anomaly is that it is deeper towards the south and shallow toward the north, and gets shallow beneath Longonot.

2.4 Discussion of Results

Magma upwelling along the Eastern Africa rift is controlled by pre-rift structures (Morley, 1994; Birt et al., 1997; Mugisha et al., 1997) and the shape of the collapse structures is influenced by the local stress field. The Longonot and Olkaria regions show interesting results where the subsurface structures define the surface volcanic features. The area around Longonot has a shallow magma system, (LR3, LR2) that is mapped to be 3km below the crater. The upwelling is noted under the crater but also towards to the northeastern side of the crater. This corresponds to a mini crater on the northern flank of the volcano. Around that edge also is the fracture zone known as the Tecto Volcanic axis, which seems to be influencing the magma uprising. The HRZ blocks are thick and we see them as crustal blocks that have been deformed by the magma through assimilation and faulting. On the Olkaria side the magma is distinct from Longonot at depths less than 10km. However at depths of 10 to 12 km, the Olkaria and Longonot magma systems appear to be connected (Figure 2.7). The magma system under Mt Longonot originates as a flattened lateral feature whose top is located 8km on the Olkaria side and at 12km on the east side. In the middle it rises up as a diapir to about 3km below surface. The diapir leans towards the east and is transected by the Tecto Volcanic axis fracture zone.

2.5 Conclusions

Using data from the MT study we are able to observe crustal features that have been faulted and subjected to active volcanism in the rift. The MT data under Mt Longonot show a large magma system that originates from greater than 8 km depth and preferentially upwells to the east. Seismic data from studies across the rift from Lake Turkana to the Kenya Dome show upper crust –lower crust boundary to be ~12km at the Mt Longonot Olkaria area (Keller et al., 1994a, 1994b; Mariita and Keller, 2007). At 12km in the Longonot region we observe a magma sill-like structure, which extends beyond the data coverage at Longonot. Results from MT data in Eburru and Olkaria show the depth to the deep magma source to be at a uniform depth of 8 km to 12 km. At Eburru the depth to the base of the deep magma is 6-8km indicating that at this

depth a sill like lenses of magma are present marking a transition between upper and lower crust. This phenomenon indicates that the crust is thinning due to extension and crustal assimilation by the intruding magma. Other volcanoes along the rift such as Silali the depth to the shallow magma is ~6km while at Menengai it is ~4km(Wamalwa and Serpa, 2013; Wamalwa et al., 2013a) and it will be interesting so find out the depth to the magma source to define the lithosphere changes with respect to the ongoing rifting.

2.6 Acknowledgements

We express thanks to KenGen for providing the all the data for this work. I especially thank Ammon Omiti, Elvis Oduong, Paul Maina and Samuel Kimani were very helpful to provide information required. We thank University of Texas at El Paso and University of Missouri for providing software to analyze the data. Thanks are due to Dr. Elizabeth Anthony who provided references and fruitful discussions about the geologic setting and volcanic activity of the East African Rift system.

2.7 References

Berdichevsky, M.N., and Dmitriev, V.I., 2008, Models and Methods of Magnetotellurics: Berlin, Heidelberg, Springer Berlin Heidelberg, doi:10.1007/978-3-540-77814-1.

Birt, C.S., Maguire, P.K.H., Khan, M.A., Thybo, H., Keller, G.R., and Patel, J., 1997, The influence of pre-existing structures on the evolution of the southern Kenya Rift Valley — evidence from seismic and gravity studies: Tectonophysics, v. 278, p. 211–242, doi:10.1016/S0040-1951(97)00105-4.

Cagniard, L., 1953, Basic theory of the magnetotelluric method of geophysical prospecting: Geophysics, v. 18, p. 605–435.

Clarke, M.C.., Woodhall, D., and Darling, G., 1990, Geological, volcanological and hydrogeological controls on the occurrence of geothermal activity in the surrounding Lake Naivasha, Kenya: British Geological Survey, 138 p.

Hersir, G.P., Arnasson, K., and Vilhjálmsson, A.M., 2015, 3D Inversion of Magnetotelluric (MT) Resistivity Data from Krýsuvík High Temperature Geothermal Area in SW Iceland: Proceedings World Geothermal Congress 2015 Melbourne, Australia, http://www.geothermal-energy.org/pdf/IGAstandard/WGC/2015/13096.pdf? (accessed May 2016).

Keller, G.R. et al., 1994a, The East African rift system in the light of KRISP 90: Tectonophysics, v. 236, p. 465–483.

Keller, G.R., Mechie, J., Braile, L.W., Mooney, W.D., and Prodehl, C., 1994b, Seismic structure of the uppermost mantle beneath the Kenya rift: Tectonophysics, v. 236, p. 201–216, doi:10.1016/0040-1951(94)90177-5.

Lemma Didana, Y., Thiel, S., and Kebede, Y., 2013, Magnetotelluric exploration at tendaho high temperature geothermal field in North East Ethiopia: ASEG Extended Abstracts, v. 2013, p. 1, doi:10.1071/ASEG2013ab110.

Mariita, N.O., and Keller, G.R., 2007, An integrated geophysical study of the northern Kenya rift: Journal of African Earth Sciences, v. 48, p. 80–94, doi:10.1016/j.jafrearsci.2006.05.008.

Martí, A., Queralt, P., and Ledo, J., 2009, WALDIM: A code for the dimensionality analysis of magnetotelluric data using the rotational invariants of the magnetotelluric tensor: Computers & Geosciences, v. 35, p. 2295–2303, doi:10.1016/j.cageo.2009.03.004.

McNeice, G.W., and Jones, A.G., 2001, Multisite, multifrequency tensor decomposition of magnetotelluric data: Geophysics, v. 66, p. 16.

Menezes, P., 2010, Magnetotellurics as a modelling tool in the extensive magmatic context of Parana Basin, Brazil: The Leading Edge, p. 832–840.

Morley, C.K., 1994, Interaction of deep and shallow processes in the evolution of the Kenya rift: Tectonophysics, v. 236, p. 81–91, doi:10.1016/0040-1951(94)90170-8.

Muchemi, G.., 1999, Conceptualised model of the Olkaria Geothermal Field: The Kenya Electricity Generating Company Ltd, 46 p.

Mugisha, F., Ebinger, C.J., Strecker, M., and Pope, D., 1997, Two-stage rifting in the Kenya rift: implications for half-graben models: Tectonophysics, v. 278, p. 63–81, doi:10.1016/S0040-1951(97)00095-4.

Onacha, S.A., 2006, Hydrothermal fault zone mapping using seismic and electrical measurements [Ph.D.]: Duke University, 226 p., https://search.proquest.com/docview/305325409/abstract/8FFEB57D7B294021PQ/4 (accessed November 2018).

Scott, S.C., 1980, The Geology of Longonot Volcano, Central Kenya: A Question of Volumes: Philosophical Transactions of the Royal Society of London. Series A, Mathematical and Physical Sciences, v. 296, p. 437–465.

Tikhonov, A.., 1950, Determination of the electrical characteristics of the deep strata of the earth's crust: Dok. Akad. Nauk. SSSR., v. 73, p. 295–297.

Wamalwa, A.M., Mickus, K.L., and Serpa, L.F., 2013a, Geophysical characterization of the Menengai volcano, Central Kenya Rift from the analysis of magnetotelluric and gravity data: GEOPHYSICS, v. 78, p. B187–B199, doi:10.1190/geo2011-0419.1.

Wamalwa, A.M., Mickus, K.L., Serpa, L.F., and Doser, D.I., 2013b, A joint geophysical analysis of the Coso geothermal field, south-eastern California: Physics of the Earth and Planetary Interiors, v. 214, p. 25–34, doi:10.1016/j.pepi.2012.10.008.

Wamalwa, A.M., and Serpa, L.F., 2013, The investigation of the geothermal potential at the Silali volcano, Northern Kenya Rift, using electromagnetic data: Geothermics, v. 47, p. 89–96, doi:10.1016/j.geothermics.2013.02.001.

White, J.C., Espejel-García, V.V., Anthony, E.Y., and Omenda, P., 2012, Open System evolution of peralkaline trachyte and phonolite from the Suswa volcano, Kenya rift: Lithos, v. 152, p. 84–104, doi:10.1016/j.lithos.2012.01.023.

Chapter 3: Dimensionality Analysis Of The Olkaria Geothermal Field, East Africa Rift

(Paper submitted for publishing to Argeo conference proceeding)

Anna W. Mwangi[1,3], Kevin Mickus[2] and Laura Serpa[1]

[1]University of Texas at El Paso, [2]Missouri State University, [3]Kenya Electricity Generating Company

awmwangi@miners.utep.edu

Keywords

Magnetotellurics, Geothermal, Dimensionality, Electrical strike

Abstract

The Olkaria geothermal field is a Quaternary rift volcano within the central region of the Kenya rift. It is a good geothermal power producer, currently generating 687.4 MWe and has much greater potential because of recent volcanic activity. Its outline is not clearly defined but structural features such as an arc of domes intersected by prominent NNS trending faults are inferred to be the edges of a collapsed caldera. Continuous geo-scientific studies designed to understand the reservoir system are vital in expanding production.

We aim to showcase geophysical results from analyzing magnetotelluric and transient electromagnetic data from Olkaria to image the subsurface. Analyses of the dimensionality from 186 magnetotelluric stations show a NE electrical strike direction for the field. Interconnected magma plutons, located about 6-7 km below the surface as depicted by low resistivity values (5 ohm-m), control the Olkaria reservoir system. The insurgence of these magma plutons seems to be structurally controlled, upwelling along weak zones becoming the loci of a high temperature hydrothermal system.

Our findings are preliminary evidence that we can map the locations and structures of the hydrothermal system. Continued analyses of these data and other geophysical information will prove new well-defined sites where hydrothermal reservoirs can best be tapped to increase the capacity of the field.

3.1 Introduction

The Olkaria geothermal prospect is located among a chain of axial volcanoes aligned along the floor of the Kenyan rift valley (Figure 1). The surface geology is characterized by comenditic lava flows and pyroclastic sequences of eruption materials from itself overlain by material exuded from neighboring Mt Longonot. Recent volcanic activity within the caldera was a fissure eruption of the Olobutot fault (280+100 years ago), covering the near terrain with an aa type rhyolitic lava flow. The subsurface geology in general is comprised of pyroclasts, rhyolites, trachytes, basalts and tuffs (Clarke et al., 1990; Omenda, 1998; Muchemi, 1999; Lagat, 2004).

Exploration of the field is challenging due to the complex geology and associated structures. There is no clear definition of a caldera margin and hence there is no clear understanding of the dynamics of the stress field, magma emplacement and subsequent eruption episodes. Geothermal wells sited at the production fields are very prolific for example there is a well pad site producing an average of 33 Mwe.

Geophysical studies applied to explore the geothermal field have been seismology, gravity, magnetic and electromagnetics. Active and passive seismic studies identified earthquake hypocenters around the field and suggest they originate from brittle/ductile interphase zones above the magma bodies (Simiyu, 1999; Simiyu and Keller, 2000; Simiyu and Malin, 2000). Mariita (2009) showed that magnetic minima indicate zones of demagnetization within the Olkaria caldera rocks and that these rocks have been heated above the Curie point temperature of 5700C. Resistivity data analysis of the region east of the domes indicate a high temperature system with a low conductivity epidote-chlorite alteration zone found at 1 km below surface (Lichoro, 2009). Additionally, hydrothermal minerals such as illite, epidote and actinolite

sampled from drill cuttings from >1km depth indicate the presence of high subsurface temperature (Karingithi, 2002; Lagat, 2004; Okoo, 2013).

Thus, the purpose of this study is to define the heat sources, the structure under the caldera, associated fault systems and to zones of hot fluid up flow, which can be tapped to produce more power. In order to investigate the geothermal subsurface structure of the Olkaria geothermal field, we used the electromagnetic methods of MT and transient electromagnetics (TEM). New MT and TEM data were combined with previously collected data with the aim of improving the electromagnetic imaging of the field. The analysis included determining the dimensionality, anisotropy and electrical strike direction of the MT data. These parameters will be used to create two-dimensional (2D) electrical models of the geothermal field.

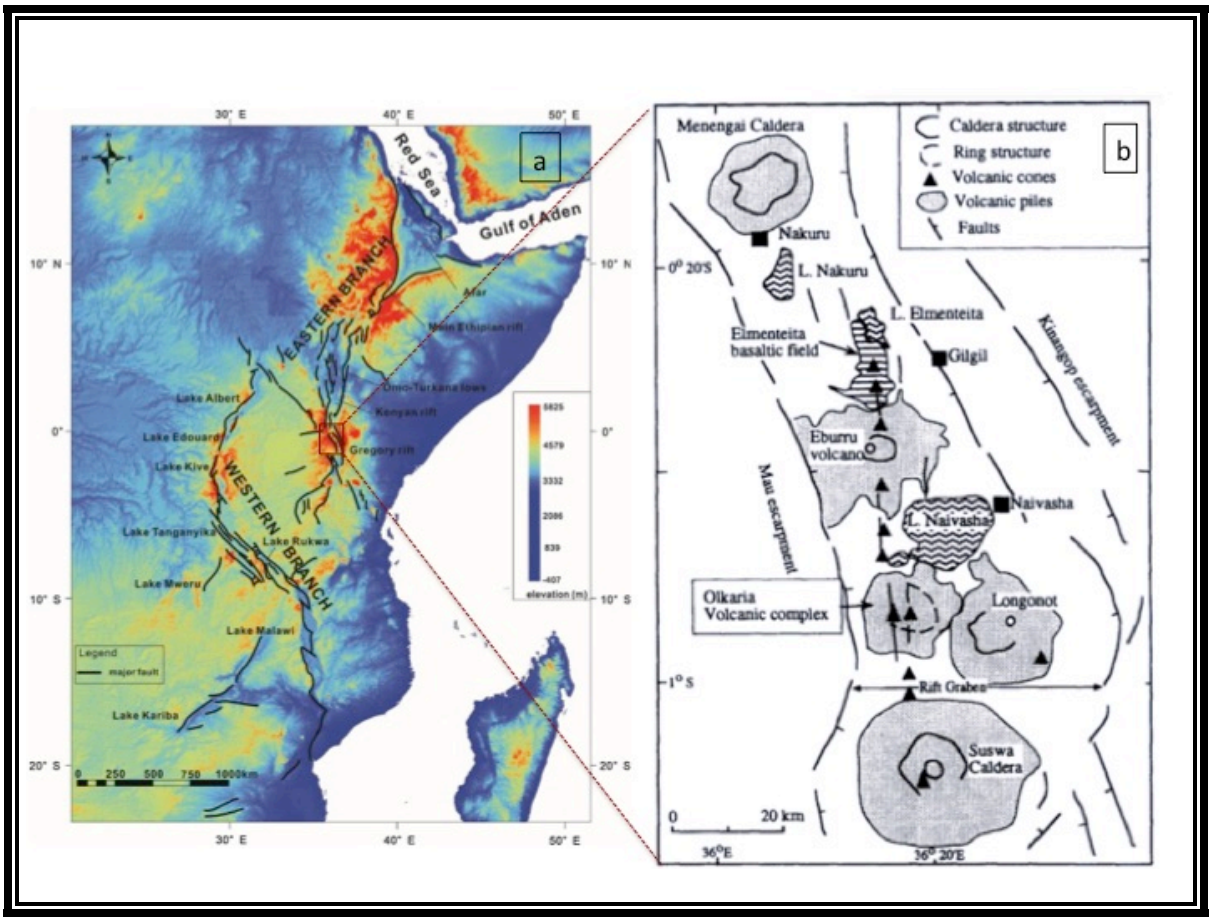

Figure 3.1: Location of the a) East Africa Rift system (Min and Hou, 2018) and b) central Kenya rift volcanoes including the Olkaria volcanic system (Omenda, 1998).

3.2 Electromagnetic Methods

Magnetotelluric methods rely on natural electromagnetic waves resulting from interaction of solar winds with earth's ionosphere and distant lightning strikes. These electromagnetic waves penetrate the earth's surface attenuating at depth where penetration depth or skin depth is dependent on the period of the wave and electrical resistivity of the subsurface material. Longer period waves will penetrate deeper into the Earth.

The central loop TEM method involves inducing an electric current along a loop into the Earth that in turn will intermittently be shut off and that decaying field induces a secondary decaying magnetic field that is measured by a receiver coil placed in the middle. From the decaying fields a voltage is induced on the receiver coil where the ground apparent resistivity values can be deduced as the eddy currents, which flow within conductors in the ground and decays characteristic of their geometry and conductance. The TEM data are used to model the near surface electrical resistivity structure and to correct the static shift problem of the MT data.

The MT data were collected as time series data and are processed in the frequency domain into electrical impedances. The electrical impedances are in a 2D Earth devolved into two perpendicular modes called the transverse magnetic (TM) and electrical (TE) modes. When the Earth is 2D, an electrical strike direction can be determined and 2D modeling can be utilized. However, most commonly the electrical structure is 3D and 2D modeling can only be used to approximate the electrical structure of a region.

To determine electrical dimensionality, the method of Martí et al. (2009) was used and to estimate the regional electrical strike direction of the data, the method of McNeice and Jones (2001) was used. The determined strike directions were then used to rotate the TM and TE data into these strike directions. The rotated TM and TE data were used to invert these data into 2D resistivity models.

3.2.1 Dimensionality Analysis of the Olkaria geothermal field

On average, the regional electrical strike direction for the Olkaria field is trending toward the NW-SE. This electrical strike direction is related to regional structural direction as evidenced

by NW-trending faults. The NW-trending fault system may influence geothermal fluids locally where conductive ions are preferentially deposited along fluid pathways; hence their alignment will be higher within fracture zones than at the low permeable zones of the rock.

Different period bands in an MT tensor off diagonal elements often show different strike orientations and these directions depend on the dominant influencing structure at that depth. The regional electrical strike was estimated for different period bands, which show different electrical strike orientations. Thus, this will indicate dominant influencing structures at different depths. We show this by plots of the electrical strike values and the associated dimensionality of each sounding were plotted at different period bands (Figure 2). At periods between 0.1 second to 1 second, the results show some areas are 1D while there are regions that are 2D and the 3D areas are scattered. For 3D cases however there tends to be a sort of alignment. From 1 second to 100 seconds the case is majority 3D with a few cases of 2D occurring in a linear fashion (Figure 2: T=1-10 sec, T=10-100sec). The dimensionality analysis of Olkaria volcanic complex is similar to that of Menengai caldera located further north of Olkaria as shown by Wamalwa et al. (2013). Both volcanoes show a 3D structure at long periods and at short periods they show a mixture of 1D, 2D and 3D trends. Moreover, both periods show clear alignment of the electrical strike and fault orientations.

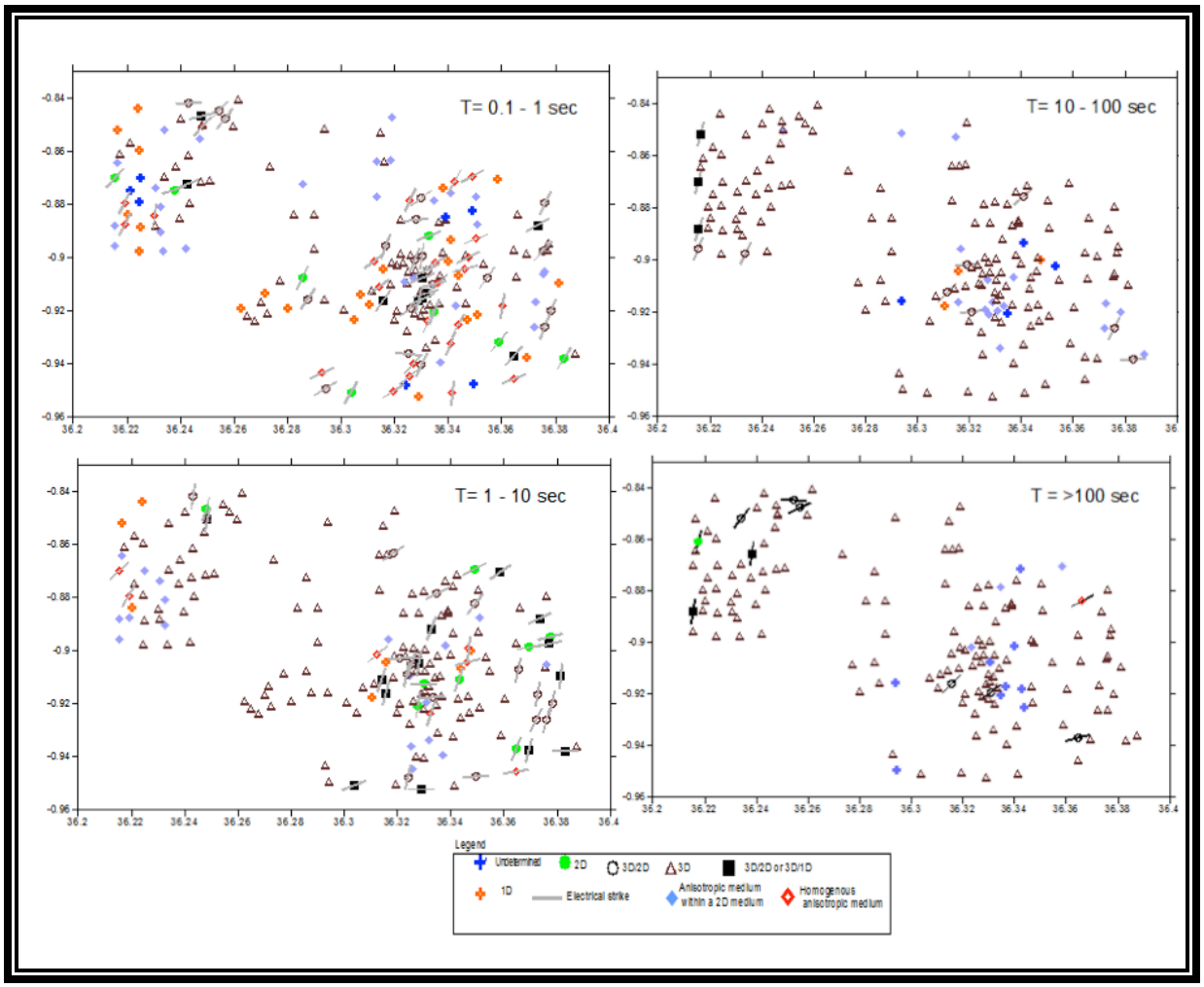

Figure 3.2: Dimensionality of Olkaria geothermal field, the points are MT sounding locations; various symbols show dimensionality type. The coordinate values: - latitude (x axis) and longitude (y axis) in degrees.

3.3 Results

The above dimensionality and regional strike analysis was used to rotate the TM and TE MT data into a preferred orientation in order to create 2D inversion models. Two profiles that cross the geothermal system were inverted. The data were static shift corrected using the TEM data, bad data were removed and the data smoothed. Figure 3 shows the location of two profiles modeled.

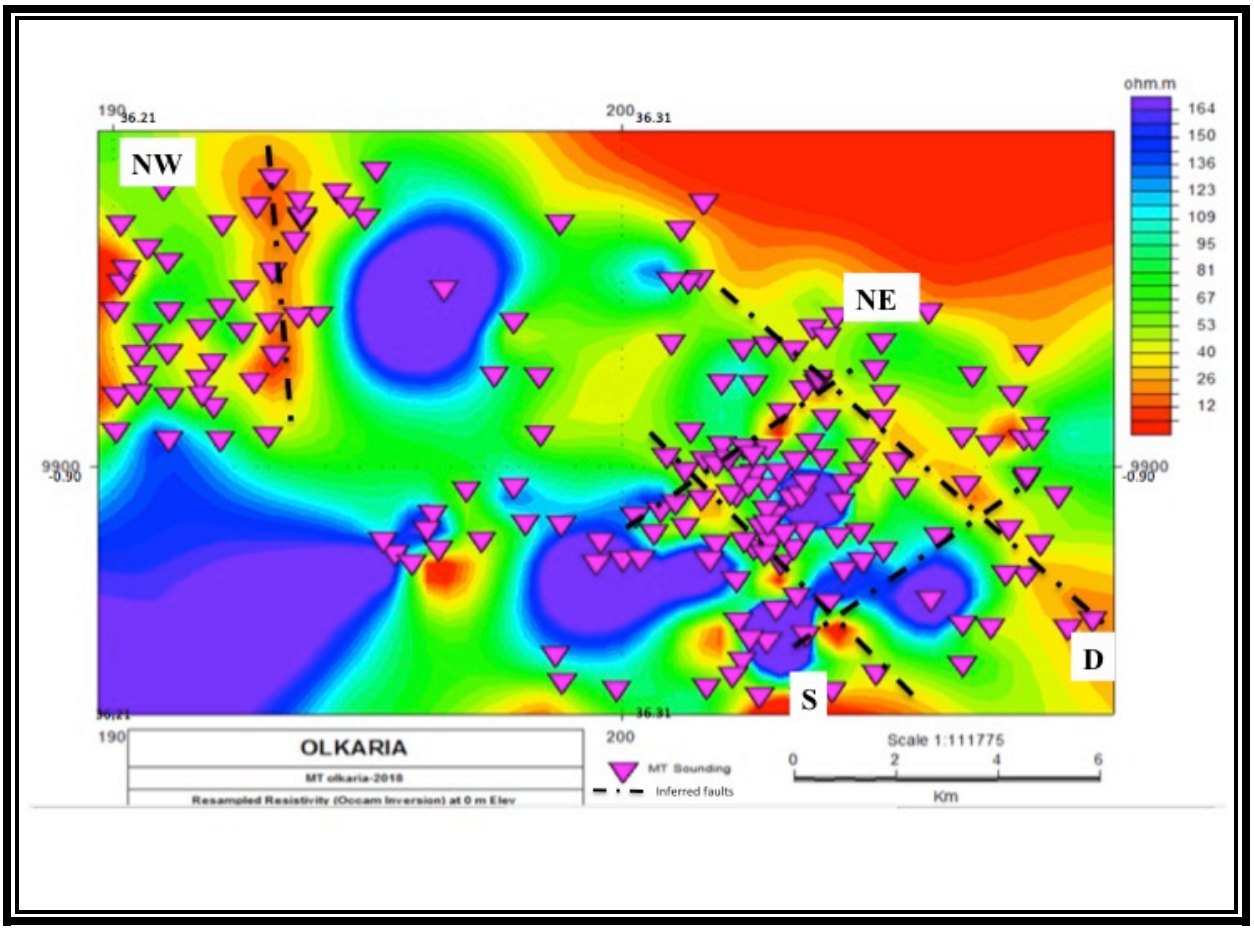

Figure 3.3: Resistivity slice at sea level approximately 2km depth from the surface. NW-D and S-NE profiles are the locations of two MT inverse models. The triangles are the location of MT stations. Dashed lines are faults. (UTM (km) and latitude – longitude (degrees) coordinates)

Final inverse models of profiles S-NE and NW-D are shown in Figure 4 and Figure 5 respectively. For each profile, several models were created where the inversion parameters and starting models were varied in order to create a model that was consistent with the observed data. The electrical resistivity cross sections show low resistivity at depths below 4-5 km, which we interpreted as the magma intrusion or a high heat zone, the heat source for the geothermal system.

The morphology of the heat source shows that it is interconnected with a deep magma pluton 16km deep. Upwelling of the shallow magma is along SSW direction and seems to be structurally controlled as it aligns with the inferred NE trending faults (Figure 3). Its morphology

is such the shallow magma chamber is elongated along NW direction as seen in Figure 4 while Figure 5 shows its cross section in the NW direction. The shape of the low conductive cap rock indicates a doming high resistivity core coinciding with high doming elevated surface.

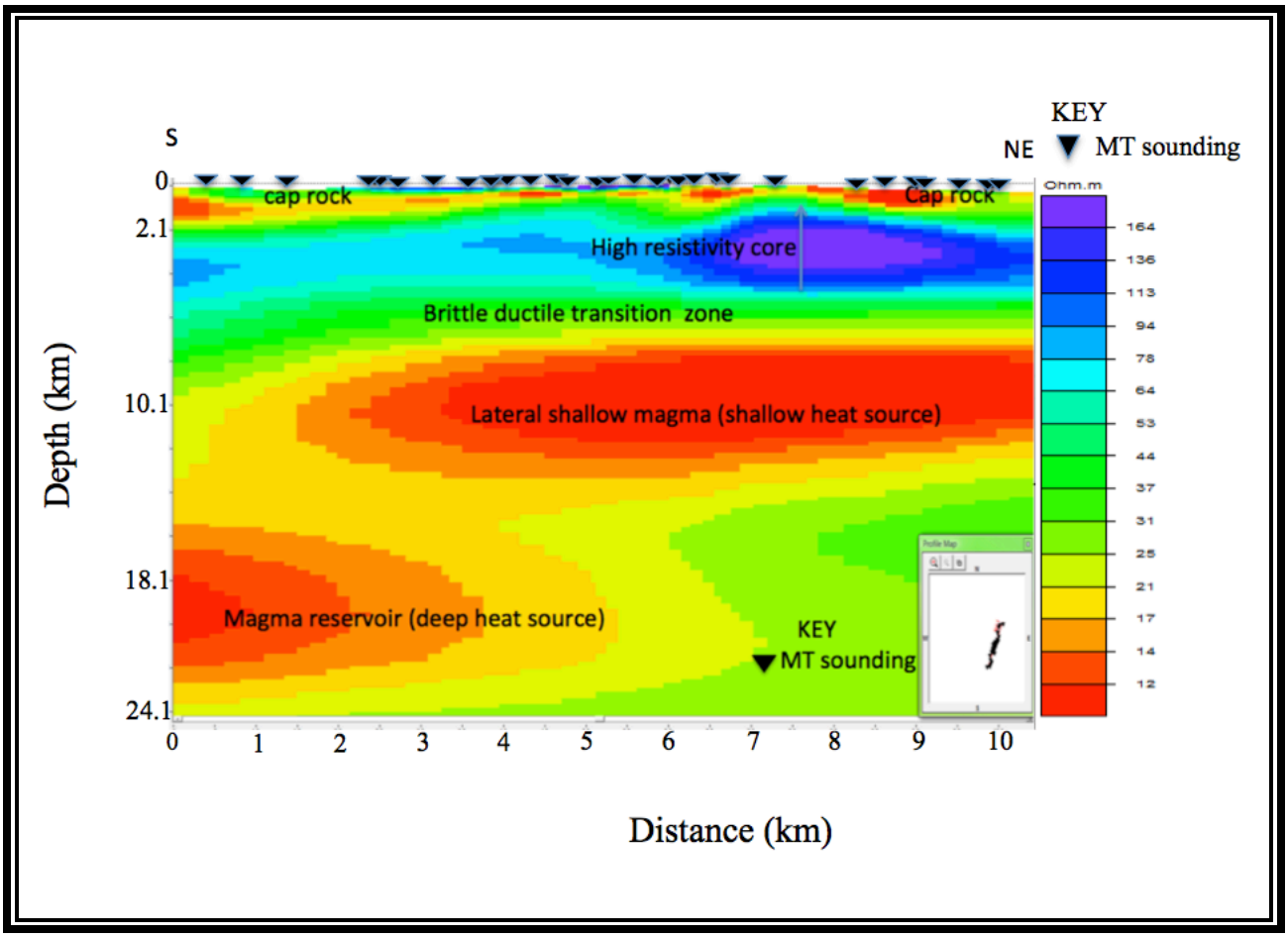

Figure 3.4: 2D inverse model along profile S-NE (Figure 3). The deeper high resistivity values are interpreted as high heat values above the magma chamber. The shallow magma intrusion is mapped at 6-7 km deep, the blue arrow shows peak of a doming resistivity core with doming elevation at the surface.

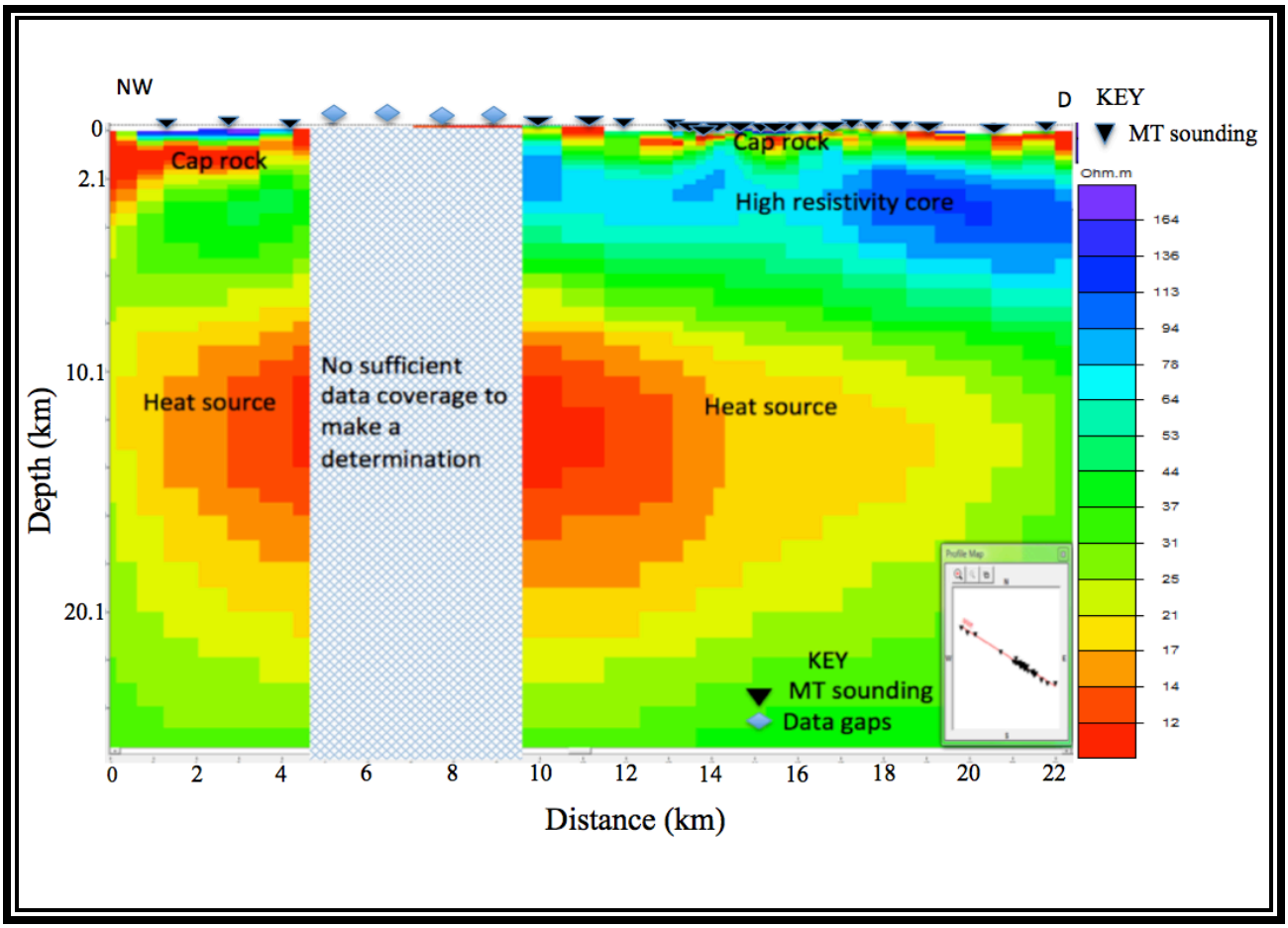

Figure 3.5: 2D inverse model along profile NW-D (Figure 3). The deeper low resistivity values are interpreted to be heat values above the magma chamber with an absence of the high resistivity core on the NW sector. The magma intrusion is mapped at 6-7 km deep.

3.3 Discussions and conclusions

A typical high resistivity core is observed directly above the heat source (55-70 ohm-m), and it is seen as a prolific reservoir zone. High temperature geothermal fields for example Krafla (Arnason and Karlsdottir, 1996) and Silali volcano (Wamalwa and Serpa, 2013; Lichoro, 2013) show a rise in resistivity in the rocks above a magma heat source. A cap rock of mixed clays (20 ohm-m) is observed overlain by a conductive smectite-zeolite minerals zone (10 ohm-m), the top of the cap rock in Figure 4 and Figure 5 and this seals the geothermal system.

The electrical resistivity response over a geothermal is distinct, because hydrothermal activity changes the host rock by dissolution or alteration of primary minerals and deposition of

secondary minerals. Alteration minerals hence can be used as temperature analogues and, moreover, they have distinct resistivity signatures. Clay minerals such as smectite and zeolites have low resistivity and are formed at low temperatures.

Figure 6 indicates different alteration minerals with their associated formation temperature and resistivity values as observed in high temperature geothermal system. Electrical conduction in the unaltered rocks is determined by pore fluid present in the rocks. At low temperatures, the zeolite smectite zone and at the geothermal cap mainly comprised mixed clays minerals, electrical conductance is determined by minerals present. At deep zones where the temperature is high, chlorite and chlorite epidote zones, resistivity is influenced by pore fluid present (Arnason et al., 2000).

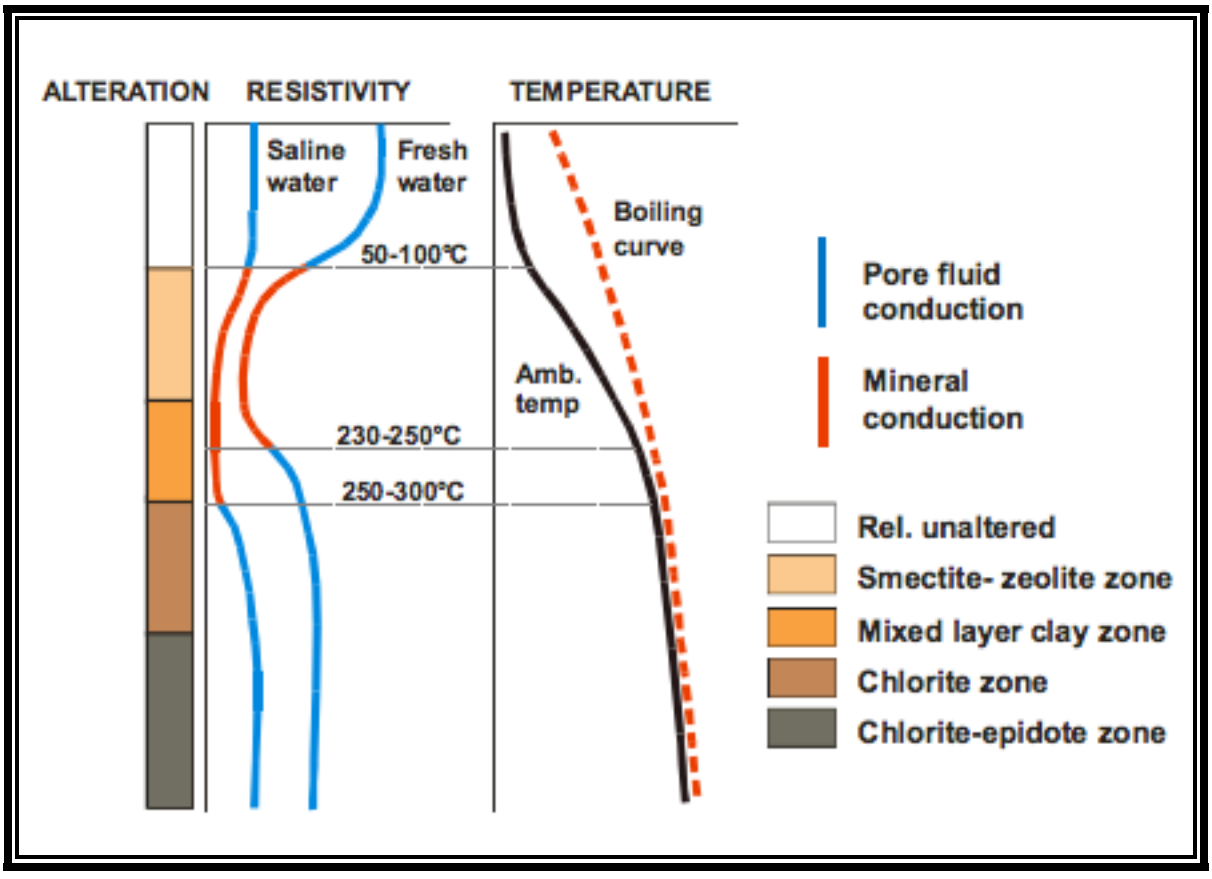

Figure 3.6: Generalized resistivity and temperature response over hydrothermally altered basaltic crust in Iceland (Flovenz et al., 1985)

A preliminary analysis of the MT data in the form of dimensionality, regional electrical strike directions and 2D inverse models shows that the orientation of the heat source of the geothermal system aligns with the determined electrical strike direction at deeper depths with the probability of being part of the regional structure impacting the dimensionality. 2D inverse models show the interconnected magma chamber or high heat source at a depth of about 6 km, which roughly agrees with the deepest observed hypo-central depths of 4 km (Simiyu and Malin, 2000).

Analysis of the MT data indicates that the transition zone is located between 4-6 km depths hence, a validation of the two geophysical techniques. The geothermal system is young, well logs show high temperature indicator minerals like epidote occur at > 1 km depth and we observe from electrical resistivity models indications of high heat denoted by high resistivity core from 1.2 km depth.

Area D in Figure 4 is the domes region and the high resistivity core shows up doming, moreover, the surface is also elevated. We attribute this to a magma emplacement process and the high resistivity-high temperature zone seems to be the up flow zone (see blue arrow). We observe the low resistivity cap rock above this high temperature is dipping and getting thicker at the edges due to deposition of conductive clays. Also at depth the interconnectivity of the magma at depth in S-NE profiles mirrors the arched domes structure on the surface and we think we are roughly observing a side view part of the caldera wall. The dimensionality analysis showed the data is 3D and this is supported by the 3D nature of the underlying major structures.

This in essence shows a vibrant geothermal system in a young rift environment and our continued work will contribute to understand its volcanic evolution, definition as well as risk management in that Biggs et al. (2009) observed characteristic inflation and deflation of the Kenya rift volcanoes including those near Olkaria.

3.4 Recommendations

We recommend ways to improve electromagnetic data acquisition within the field.

• Cultural noise is prevalent in the Olkaria field stemming from the ongoing development including from electricity transmission. This results in low quality MT and TEM data near electrical installations. A speedy effort for electromagnetic data acquisition in areas with no data should be prioritized before permanent structures/activities are installed.

• To image deeper into the earth an average of 30 hours acquisition time is ideal to resolve both local and regional structures.

• Other geophysical methods such as continuous seismic data monitoring is essential to monitor volcanic activity as well constrain of electromagnetic geophysical models proposed.

3.5 References

Arnason, K., and Karlsdottir, R., 1996, A TEM resistivity survey of the Krafla high-temperature field: OS-96005/JHD-03, 96p.

Arnason, K., Karlsdottir, R., Eysteinsson, H., Flovenz, O.G., and Gudlaugsson, S.T., 2000, The Resistivity Structure Of High-Temperature Geothermal Systems In Iceland, in Kyushu Japan, p. 6.

Biggs, J., Anthony, E.Y., and Ebinger, C.J., 2009, Multiple inflation and deflation events at Kenyan volcanoes, East African Rift: Geology, v. 37, p. 979–982.

Clarke, M.C., Woodhall, D., and Darling, G., 1990, Geological, volcanological and hydrogeological controls on the occurrence of geothermal activity in the surrounding Lake Naivasha, Kenya: British Geological Survey, 138 p.

Flovenz, O.G., Georgesson, L., and Arnason, K., 1985, Resistivity Structure of the upper crust in Iceland: v. 90-B12, p. 10,136-10,150.

Karingithi, C.W., 2002, Hydrothermal Mineral Buffers Controlling Reactive Gases Concentration In The Greater Olkaria Geothermal System, Kenya: United Nations University- Geothermal training Programme, 61 pp.

Lagat, J.K., 2004, Geology, Hydrothermal Alteration And Fluid Inclusion Studies Of Olkaria Domes Geothermal Field, Kenya: United Nations University- Geothermal training Programme, 79 pp.

Lichoro, C., 2009, Joint 1-D Inversion of TEM And MT Data from Olkaria Domes Geothermal Area, Kenya: United Nations University- Geothermal training Programme, 289–318 p.

Lichoro, C.M., 2013, Multi-Dimensional Interpretation of Electromagnetic Data From Silali Geothermal Field In Kenya: Comparison Of 1-D, 2-D and 3-D Mt Inversion: United Nations University- Geothermal training Programme, 30 pp.

Mariita, N.O., 2009, Application of Geophysics to Geothermal energy exploration and monitoring of its exploitation: Short Course IV on Exploration for Geothermal Resources, organized by. UNU-GTP, KenGen and GDC, at Lake Naivasha, Kenya (November 1-22), 9 pp.

Martí, A., Queralt, P., and Ledo, J., 2009, Waldim: A code for the dimensionality analysis of magnetotelluric data using the rotational invariants of the magnetotelluric tensor: Computers & Geosciences, v. 35, p. 2295–2303.

McNeice, G.W., and Jones, A.G., 2001, Multisite, multifrequency tensor decomposition of magnetotelluric data: Geophysics, v. 66, p. 16.

Min, G., and Hou, G., 2018, Geodynamics of the East African Rift System ~30 Ma ago: A stress field model: Journal of Geodynamics, v. 117, p. 11 pp.

Muchemi, G., 1999, Conceptualised model of the Olkaria Geothermal Field: The Kenya Electricity Generating Company Ltd, 46 p.

Okoo, J., 2013, Borehole Geology And Hydrothermal Alteration Mineralogy Of Well Ow-39a, Olkaria Geothermal Project, Naivasha, Kenya: United Nations University- Geothermal

training Programme 24, 574–576 p., http://os.is/gogn/unu-gtp-report/UNU-GTP-2013-24.pdf.

Omenda, P.A., 1998, The Geology And Structural Controls of The Olkaria Geothermal System, Kenya: Geothermics, v. 27, p. 55–74.

Simiyu, S.M., 1999, Seismic Velocity Analysis in the Olkaria Geothermal Field, in Stanford, California,v.SGP-TR-162,p.7.

Simiyu, S.M., and Keller, G.R., 2000, Seismic monitoring of the Olkaria Geothermal area, Kenya Rift valley: Journal of Volcanology and Geothermal Research, v. 95, p. 197–208.

Simiyu, S.M., and Malin, P.E., 2000, A "Volcanoseismic" Approach To Geothermal Exploration And Reservoir Monitoring: Olkaria, Kenya And Casa Diablo, Usa: Proceedings World Geothermal Congress 2000 Kyushu - Tohoku, Japan, p. 1759–1763.

Wamalwa, A.M., Mickus, K.L., and Serpa, L.F., 2013, Geophysical characterization of the Menengai volcano, Central Kenya Rift from the analysis of magnetotelluric and gravity data: Geophysics, v. 78, p. B187–B199.

Wamalwa, A.M., and Serpa, L.F., 2013, The investigation of the geothermal potential at the Silali volcano, Northern Kenya Rift, using electromagnetic data: Geothermics, v. 47, p. 89–96.

Vita

Anna Wairimu Mwangi was born in Nairobi, Kenya on 5th August 1983. She is the 3rd born among 3 boys, the daughter of John Mwangi Nduati and Mary Wambui Mwangi. She attained a BSc. in Geology in 2006 and went on to pursue MSc. in Applied Geophysics at the University of Nairobi the same year and completed in 2012. In November 2008 she got employed by Kenya Electricity Generating Company as a Geophysicist and got promoted to a Senior Geophysicist position in 2009. She worked in various geothermal prospects around the Kenyan Rift valley, exploring for geothermal resources. In addition, she did consultancy work exploring for geothermal resources in Rwanda's Karisimbi volcano and Bayuda province in Sudan. In 2013 she was accepted at the University of Texas at El Paso to pursue a Doctoral program in Geology (Geophysics major). Her thesis work involves exploration of the central Kenya rift volcanoes using electromagnetic methods for the purpose of geothermal development. In the course of the studies she presented her work at various conferences and published a conference paper. She plans to publish the work in this dissertation to a scientific journal. She plans to work in the energy sector in Kenya playing a role in the exploration and management of subsurface energy reservoirs.

Email: anna.mwangi@gmail.com

This dissertation was typed by Anna Wairimu Mwangi.